

Subunit-selective proteasome activity profiling uncovers uncoupled proteasome subunit activities during bacterial infections

Johana C. Misas-Villamil^{1,2}, Aranka M. van der Burgh^{1,8}, Friederike Grosse-Holz⁷, Marcel Bach-Pages⁷, Judit Kovács^{1,6}, Farnusch Kaschani³, Sören Schilasky¹, Asif Emron Khan Emon^{1,4}, Mark Ruben⁵, Markus Kaiser³, Hermen S. Overkleeft⁵, and Renier A. L. van der Hoorn^{1,7*}

¹ The Plant Chemetics Laboratory, Max Planck Institute for Plant Breeding Research, Carl-von-Linné Weg 10, 50829 Cologne, Germany

² Botanical Institute and Cluster of Excellence on Plant Sciences, University of Cologne, 50674 Cologne, Germany

³ Chemical Biology, Universität Duisburg-Essen, Zentrum für Medizinische Biotechnologie, Fakultät für Biologie, Universitätsstr. 2, 45117 Essen, Germany

⁴ Current address: Bonn-Aachen International Center for IT, University of Bonn, Dahlmannstrasse 2, 53113 Bonn, Germany

⁵ Institute of Chemistry and Netherlands Proteomics Centre, Gorlaeus Laboratories, 2333 CC Leiden, The Netherlands

⁶ Department of Plant Biology, University of Szeged, Szeged, Hungary

⁷ The Plant Chemetics Laboratory, Department of Plant Sciences, University of Oxford, South Parks Lane OX1 3RB Oxford, United Kingdom

⁸ Current address: Laboratory for Phytopathology, Wageningen University, Droevendaalsesteeg 1, 6708 PB Wageningen, The Netherlands.

*, for correspondence: renier.vanderhoorn@plants.ox.ac.uk

Keywords: catalytic subunit; core protease; *Arabidopsis thaliana*; *Nicotiana benthamiana*; Activity-based protein profiling; proteasome manipulation.

Running head: Subunit-selective proteasome activity profiling

Significances Statement: Proteasome activity profiling with subunit-selective fluorescent probes is a robust way to display activities of $\beta 1$ and $\beta 5$ activities in any plant species. We validate these next generation tools and use it to uncover that $\beta 1$ and $\beta 5$ activities are uncoupled upon infection by virulent bacteria.

SUMMARY

The proteasome is a nuclear - cytoplasmic proteolytic complex involved in nearly all regulatory pathways in plant cells. The three different catalytic activities of the proteasome can have different functions but tools to monitor and control these subunits selectively are not yet available in plant science. Here, we introduce subunit-selective inhibitors and dual-color fluorescent activity-based probes for studying two of the three active catalytic subunits of the plant proteasome. We validate these tools in two model plants and use this to study the proteasome during plant-microbe interactions. Our data reveals that *Nicotiana benthamiana* incorporates two different paralogs of each catalytic subunit into active proteasomes. Interestingly, both $\beta 1$ and $\beta 5$ activities are significantly increased upon infection with pathogenic *Pseudomonas syringae* pv. *tomato* DC3000 lacking hopQ1-1 (PtoDC3000(Δ hQ)) whilst the activity profile of the $\beta 1$ subunit changes. Infection with wild-type PtoDC3000 causes proteasome activities that range from strongly induced $\beta 1$ and $\beta 5$ activities to strongly suppressed $\beta 5$ activities, revealing that $\beta 1$ and $\beta 5$ activities can be uncoupled during bacterial infection. These selective probes and inhibitors are now available to the plant science community and can be widely and easily applied to study the activity and role of the different catalytic subunits of the proteasome in different plant species.

INTRODUCTION

The ubiquitin proteasome pathway is responsible for the selective degradation of proteins in the cell regulating numerous cellular and physiological functions. The proteasome is a multi-subunit, ATP-dependent proteolytic complex consisting of a 20S core particle (CP) and a 19S regulatory particle (RP) (Groll et al., 1997). The CP is ubiquitin and ATP independent, and consists of four stacked rings forming a barrel. The inner two rings of the barrel consist of β subunits and these are flanked by two rings of α subunits (Kurepa and Smalle, 2008a). Each ring consists of seven subunits. The catalytic subunits responsible for peptide cleavage are located in the β rings and have an active site N-terminal Threonine (Thr). The catalytic β subunits have different proteolytic activities: $\beta 1$ has caspase-like activity, $\beta 2$ trypsin-like activity and $\beta 5$ chymotrypsin-like activity (Dick et al., 1998).

In addition to its crucial role in plant hormone signaling, the ubiquitin proteasome pathway has received attention in the plant pathogen field because several pathogens target this system. The proteasome acts as a hub in various immune signalling cascades, and is therefore an obvious target for pathogens (Üstün et al., 2016). Pathogen-derived effectors were found to interact with components of the ubiquitin proteasome system such as E3-ligases, F-box proteins and SUMO de-conjugation enzymes (Banfield et al., 2015). These effectors interfere in vesicle trafficking or promote transcription factor degradation. Some of these bacterial effectors act by inhibiting the proteasome. For instance, the XopJ effector produced by *Xanthomonas campestris* pv. *vesicatoria* and the HopZ4 effector from *Pseudomonas syringae* pv. *lachrymans* interact with the RPT6 subunit of the 19S regulatory particle, suppressing the activity of the proteasome and repressing salicylic acid (SA)

mediated responses (Üstün et al., 2013; 2014). In addition, the non-ribosomal polypeptide Syringolin A (SylA) secreted by *Pseudomonas syringae* pv. *syringae* also targets the proteasome (Groll et al., 2008), in this case by covalently inhibiting $\beta 2$ and $\beta 5$ subunits of the plant proteasome (Kolodziejek et al. 2011). SylA facilitates opening of stomata and promotes bacterial colonization from wound sites (Misas-Villamil et al., 2013; Schellenberg et al., 2010).

So far, the plant proteasome could not be sufficiently investigated due to technical limitations and lack of suitable approaches. First, reverse genetic approaches are challenging since mutations in CP subunits usually cause severe pleiotropic defects or even lethality (Kurepa and Smalle, 2008a). Roles of the different CP subunits are also impossible to study using a knockout approach since the CP requires integrity for its function. Second, a number of proteasome subunits are modified post-translationally, e.g. by proteolytic processing, acetylation and ubiquitylation (Book et al., 2010). Third, the proteasome is a versatile complex in which substrate specificities can be changed, depending on the assembly of the different subunits. The most notable example is the immunoproteasome in mammals in which constitutive subunits of the CP are replaced by inducible subunits (Aki et al., 1994). The recently discovered replacement of $\alpha 3$ by $\alpha 4$ in human proteasomes is another example of alternative proteasomes (Padmanabhan et al., 2016). Although there is no evidence that plants have an alternative proteasome, plant genomes carry multiple genes for nearly each subunit (Yang et al., 2004) and the proteasome in *Arabidopsis* is assembled with paralogous pairs for most subunits (Book et al., 2010). Remarkably, tobacco genes encoding $\beta 1$, $\alpha 3$ and $\alpha 6$ subunits are transcriptionally upregulated after treatment with the elicitor cryptogein (Suty et al., 2003) indicating that plants might assemble inducible alternative proteasomes.

The activity of the proteasome subunits can be studied using fluorogenic substrates, which require the isolation and purification of the proteasome, a very tedious and laborious method only applicable on certain soft plant tissues (Yang et al., 2004; Book et al., 2010). We previously introduced activity-based protein profiling (ABPP) to monitor the activity of the plant proteasome (Gu et al., 2010). ABPP relies on the use of small molecule chemical probes that are composed of a reactive group, a linker and a reporter tag that can be biotin or fluorescent to facilitate protein purification and detection, respectively (Cravatt et al., 2008). These chemical probes react with the active site of enzymes, resulting in a covalent and often irreversible labeling, which facilitates the detection, purification and identification of those labeled proteins. Labeling reflects protein activity rather than abundance because the probes only react when the active site is available and reactive and many enzymes are regulated by changes in the availability and reactivity of the active site. So far we have introduced over 40 activity-based probes into plant science to monitor e.g. Cys proteases, glycosidases, subtilases, acyltransferases and glutathione transferases, and many of these probes are widely used in plant science (Morimoto and Van der Hoorn, 2016). DCG-04, for instance, is a probe for papain-like Cys proteases (Greenbaum et al., 2000; Van der Hoorn et al., 2004) that has been instrumental for the discovery of pathogen-derived inhibitors (Rooney et al., 2005; Tian et al., 2007;

Shabab et al., 2008; Van Esse et al., 2008; Song et al., 2009; Kaschani et al., 2010; Lozano-Torres et al., 2012; Mueller et al., 2013), deciphering protease-inhibitor arms-races and effector adaptation upon a host jump (Hörger et al., 2012; Dong et al., 2014), and identifying senescence-associated proteases (Martinez et al., 2007; Carrion et al., 2013; Porret et al., 2015). Likewise, proteasome probes have been used to describe post-translational activation of the proteasome during salicylic acid signaling (Gu et al., 2010), the selective suppression of the nuclear proteasome by bacterial phytotoxin Syringolin A (SylA, Kolodziejek et al., 2011; Misas-Villamil et al., 2013); and the regulation of the proteasome by NAC transcription factor RPX (Nguyen et al., 2013), the validation and availability of next generation chemical probes will underpin exciting scientific discoveries.

The activity of the three catalytic subunits of the Arabidopsis proteasome can be easily distinguished using ABPP since these subunits have different molecular weight (MW) (Gu et al., 2010; Kolodziejek et al., 2011). In other plants, however, the MW of these different subunits can overlap and multiple subunit genes can cause additional signals that are difficult to annotate (Gu, 2010). In the model plant *Nicotiana benthamiana*, for instance, all three different catalytic subunits were detected in a single band (Misas-Villamil et al., 2013). Here, we describe subunit-specific labeling for two catalytic subunits. By using these next generation probes we are able to display activities of $\beta 1$ and $\beta 5$ catalytic subunits in *N. benthamiana*, revealing that activity of these subunits independently change upon bacterial infection.

RESULTS

LW124 and MVB127 are selective probes for the $\beta 1$ and $\beta 5$ catalytic subunits

We have previously used MVB072 (**Figure 1a**), a probe that labels all three catalytic subunits of the plant proteasome (Kolodziejek et al., 2011). Labeling of Arabidopsis leaf extracts with MVB072 results in three signals representing $\beta 2$ (top band 1), $\beta 5$ (middle band 2) and $\beta 1$ (bottom band 3) (**Figure 1b**, Kolodziejek et al., 2011). We also have previously introduced a rhodamine-tagged SylA (RhSylA, **Figure 1a**) which preferentially labels $\beta 2$ (top band 6), and $\beta 5$ (bottom band 7) (**Figure 1b**, Kolodziejek et al., 2011).

Here we introduce two next generation probes for labeling of specific proteasome catalytic subunits. LW124 contains an epoxyketone reactive group, the tetrapeptide Ala-Pro-Nle-Leu and a bodipy Cy2 fluorescent group (**Figure 1a**, Li et al., 2013). MVB127 has a vinyl sulphone (VS) reactive group, a MeTyr-Phe-Ile tripeptide and a bodipy Cy2 fluorescent group with an azide group that can be used for click chemistry reactions (**Figure 1a**, Li et al., 2013). In contrast to MVB072 labeling, which in Arabidopsis results in three signals, we detect only one signal for LW124 at 26 kDa (**Figure 1b**, band 4), and one signal for MVB127 at ca. 27 kDa (**Figure 1b**, band 5). No strong signals appear in the remainder of the gels (Supplemental **Figure S1**). All signals are caused by proteasome labeling since they are suppressed upon pre-incubation with the selective proteasome inhibitor epoxomicin (Supplemental **Figure S2**).

Because LW124 carries a different fluorophore, we tested if these probes can be mixed and used in co-labeling experiments. Co-labeling by adding two probes at the same time and with the same concentration to Arabidopsis leaf extracts indeed shows specific signals for both probes (**Figure 1c**). The bottom signal (band 3, $\beta 1$) of MVB072 is suppressed upon co-labeling with LW124 (**Figure 1c**, lane 4), indicating that LW124 targets $\beta 1$ of the Arabidopsis proteasome. The overlay shows that the $\beta 1$ -LW124 conjugate (band 4) migrates slightly faster in the protein gel than the $\beta 1$ -MVB072 conjugate (band 3), consistent with the different MW of the two probes (**Figure 1b** and **1c**, lanes 1 and 2). A suppression of labeling cannot be observed upon co-labeling of MVB072 with MVB127 since they carry the same fluorophore (**Figure 1c**, lane 5). Co-labeling of LW124 with MVB127 results in two signals (**Figure 1c**, top two panels, lane 6), indicating that these probes label different subunits. However, the MVB127 signal (band 5) is suppressed upon colabeling with LW124 (**Figure 1c**, lanes 3 and 6). By contrast, labeling by LW124 (band 4) seems unaffected upon co-labeling with MVB127 (**Figure 1c**, lanes 2 and 6).

To confirm that LW124 and MVB127 are specific probes for one proteasome catalytic subunit, we pre-incubated the samples with subunit-specific proteasome inhibitors that have been validated on mammalian proteasomes. N3 $\beta 1$ is an epoxyketone inhibitor that targets the $\beta 1$ catalytic subunit, whereas N3 $\beta 5$ is a vinyl sulphone inhibitor of the $\beta 5$ catalytic subunit (**Figure 2a**, Verdoes et al., 2010). Notably, these are non-fluorescent versions of the probes since the peptide and reactive group (warhead) of N3 $\beta 1$ is identical to that of LW124 and the warhead of N3 $\beta 5$ is identical to that of MVB127 (**Figures 1a** and **2a**). Pre-incubation with N3 $\beta 1$ suppresses labeling of only the bottom band 3 in the MVB072 labeling profile, confirming that this inhibitor is selective for the $\beta 1$ subunit (**Figure 2b**, lane 2). By contrast, pre-incubation with N3 $\beta 5$ suppresses MVB072 labeling of the middle band 2, confirming selectivity for $\beta 5$ (**Figure 2b**, lane 3).

Having verified the selectivity of N3 $\beta 1$ and N3 $\beta 5$, we tested if LW124 and MVB127 labeling can be suppressed by the respective subunit-selective inhibitor. N3 $\beta 1$ suppresses labeling of LW124 (**Figure 2b**, lanes 5 and 8), confirming that LW124 targets $\beta 1$, consistent with the structural similarity of LW124 with N3 $\beta 1$ (**Figures 1a** and **2a**). Importantly, the suppression of MVB127 labeling by N3 $\beta 5$ (**Figure 2b**, lanes 6 and 12) shows that MVB127 targets $\beta 5$, consistent with the structural similarity of MVB127 with N3 $\beta 5$ (**Figures 1a** and **2a**). The $\beta 5$ -MVB127 conjugate (band 5) migrates slightly faster in the protein gel than the $\beta 5$ -MVB072 conjugate (band 2), consistent with the different MW of the two probes (**Figures 1b** and **1c**, lanes 1 & 3, and **2b**, lanes 1 & 4). Importantly, pre-incubation of N3 $\beta 1$ or N3 $\beta 5$ in the reciprocal combinations with the probes, did only slightly reduce MVB127 and LW124 labeling, respectively (**Figure 2b**, lanes 5, 6, 9, and 11), indicating that both inhibitors and probes are specific for their targets. Taken together these data show that LW124 and MVB127 are selective probes for $\beta 1$ and $\beta 5$ catalytic subunits, respectively.

Specific labeling of the $\beta 2$ catalytic subunit

Having established selective labeling of the $\beta 1$ and $\beta 5$ catalytic subunits, we next developed a method to monitor $\beta 2$. We previously found that RhSylA targets the proteasome subunits $\beta 2$ and $\beta 5$ at short labeling times (Kolodziejek et al., 2011). Taking advantage of this feature we tested if inhibition of the $\beta 5$ proteasome subunit using N3 $\beta 5$ together with short labeling by RhSylA will result in specific labeling of $\beta 2$. We therefore pre-incubated Arabidopsis leaf extracts with various concentrations of N3 $\beta 5$ and labeled for 30 min with 0.5 μ M RhSylA. Increasing N3 $\beta 5$ concentrations up to 5 μ M N3 $\beta 5$ reduces $\beta 5$ labeling (**Figures 3a** and **3b**). $\beta 5$ labeling remains unaltered at higher N3 $\beta 5$ concentrations (**Figures 3a** and **3b**) indicating that $\beta 5$ subunit is saturated by N3 $\beta 5$. Signal intensities derived from $\beta 1$ and $\beta 5$ at 5 μ M N3 $\beta 5$ are very faint in comparison to the $\beta 2$ signal, which remains unaffected (**Figure 3b**). This data demonstrates that RhSylA labeling in the presence of 5 μ M N3 $\beta 5$ is a suitable approach to monitor labeling of $\beta 2$.

Subunit-specific probes display multiple $\beta 1$ signals in N. benthamiana

N. benthamiana is increasingly used as a model plant to study protein regulation and localization upon transient expression. Additionally, *N. benthamiana* can be infected by a range of different pathogens, which makes this species ideal to unravel plant defense (Goodin et al., 2008). Labeling of *N. benthamiana* leaf extracts with MVB072 results in two signals: one strong signal at 28 kDa and one faint signal at ca. 27 kDa (**Figure 4a**, lane 1, bands 1 and 2, Misas-Villamil et al., 2013). MS analysis of the MVB072-labeled proteins representing the major signal revealed that it contains $\beta 1$, $\beta 2$ and $\beta 5$ subunits (Misas-Villamil et al., 2013). Thus, in contrast to Arabidopsis where the three catalytic subunits cause three distinct signals, the *N. benthamiana* proteasome subunits cannot be distinguished by MVB072 labeling because the signals overlap.

To monitor the catalytic subunits of the *N. benthamiana* proteasome, we tested the subunit-selective probes. Surprisingly, LW124 labeling displays two 27 kDa signals, indicating that there might be two different subunits labeled by LW124 in *N. benthamiana* (**Figure 4a**, lane 2, bands 3 and 4). Co-labeling of MVB072 with LW124 shows two signals for LW124 and one signal for MVB072 (**Figure 4a**, lane 4 overlay). The weak bottom MVB072 signal (band 2) is absent upon co-labeling with LW124, indicating that this signal is caused by $\beta 1$. Because the top MVB072 signal (band 1) also contains $\beta 1$ (Misas-Villamil et al., 2013), both MVB072 signals contain $\beta 1$, consistent with the two signals displayed by LW124. The overlay, however, shows that the two MVB072 signals migrate slower in the gel than the two LW124 conjugates (**Figure 4a**, lanes 1 and 2), which is consistent with the MW shift seen for Arabidopsis, and is explained from the fact that MVB072 is larger and more bulkier when compared to LW124 (**Figures 1a** and **2a**).

MVB127 labeling shows one specific signal at 28 kDa (**Figure 4a**, lane 3, band 5). Co-labeling of MVB072 with MVB127 causes a more intense bottom signal, caused by an overlap of the $\beta 1$ -MVB072 and $\beta 5$ -MVB127 conjugates. The observation that the $\beta 5$ -MVB127 conjugate migrates faster through the protein gel than the $\beta 5$ -MVB127 conjugate is consistent with the MW shift seen for

Arabidopsis, and is explained from the fact that MVB072 is larger and more bulkier when compared to MVB127 (**Figures 1a and 2a**). LW124 and MVB127 co-labeling results in two signals for LW124 and one signal for MVB127 (**Figure 4a**, lane 6).

Pre-incubation with N3 β 1 and N3 β 5 confirms that the lowest MVB072 signal (**Figure 4b**, band 2) and the two LW124 correspond to β 1 (**Figure 4b**, bands 3 and 4), whereas the MVB127 signal corresponds to β 5 (**Figure 4b**, band 5), supporting the specificity of β 1 and β 5 labeling by LW124 and MVB127, respectively (**Figure 4b**, lanes 5-12). There is, however, some reciprocal suppression of N3 β 1 on MVB127(β 5) and N3 β 5 on LW124(β 5) (**Figure 4b**, lanes 5, 6, 9 and 11).

Phylogenetic and proteomic analysis reveals multiple incorporated proteasome subunits in N. benthamiana

The detection of two β 1 signals in *N. benthamiana* using LW124 is remarkable, since the Arabidopsis genome has only one gene encoding β 1, and *β 1din* in tobacco is defence induced (Suty et al., 2003). We therefore searched the *N. benthamiana* genome (<https://solgenomics.net/>) for genes encoding catalytic subunits of the proteasome. Blast searches for catalytic subunits resulted in six predicted β 1 proteins, three β 2 proteins and three β 5 proteins. Phylogenetic analysis revealed that the paralogous subunits are more related to each other than to the subunits of Arabidopsis, except for β 1, where two groups seem to exist in *N. benthamiana* (**Figure 5**). One β 1 and one β 2 subunit are shorter than their respective paralogs. We consider these pseudogenes since their predicted MW is too low to explain the signals we detect upon labeling.

To determine if these genes also encode for proteins that are part of the active proteasome in leaves, we performed mass spectrometry analysis of two different pull down experiments of *N. benthamiana* leaf extracts labeled with MVB072. To also detect an altered subunit assembly during defence, the pull down was performed on plants treated with the SA analog benzothiadiazole (BTH), whereas the other pull down was performed on the mock control. Each pull down assay was analyzed twice by MS and 45 peptides were detected of the catalytic subunits, of which 11 were unique (Supplemental **Table S1** and **Figure S3**).

In these experiments we identified unique peptides of two different β 1 subunits: β 1a and β 1b (**Figures 5b, 5c and S2**). Several peptides that are shared with one other protein (dark grey) map to the truncated β 1 subunit (NbS00011733g0005.1) (dark grey in **Figure 5c**). The truncated subunit would migrate at a predicted 16.7 kDa, but we do not detect fluorescent signals in this region. Removal of this subunit from the analysis would add two additional unique peptides to one of the already identified β 1a subunit (NbS0009991g0103.1). The presence of two β 1 subunits having a different predicted MW of 23.7 (β 1a) and 22.6 (β 1b) kDa is consistent with the two LW124 signals detected upon labeling.

We also detected unique peptides for two β 2 subunits (β 2a and β 2b) and one β 5 subunit (β 5a) (**Figure 5b**). Two other β 5 subunit peptides do not match to this identified β 5a protein, indicating that

there must be a second $\beta 5$ subunit ($\beta 5b$), which is either Nb00003340g0007.1 or the shorter NbS00002498g0003.1 (**Figures 5b** and **5c**). These findings confirm an expanded repertoire of catalytic proteasome subunits in active proteasomes of *N. benthamiana*.

Comparison of the identified proteasome subunits from water- and BTH-treated plants did not reveal significant differences (**Figure 5b**). These data suggest that the active catalytic proteasome subunit incorporation is not different during SA-induced defence. However, more quantitative proteomic analysis with more samples may be required to rule out any changes upon BTH treatment.

Bacterial infections affect active subunit composition in N. benthamiana.

We next used the subunit-selective probes to investigate changes in the proteasome subunit composition during biotic stress. We therefore infected *N. benthamiana* leaves with *P. syringae* pv. *tomato* DC3000 (PtoDC3000), which triggers a non-host response (NHR, or effector-triggered immunity (ETI)) because it produces type-III effector hopQ1-1, which is recognized in *N. benthamiana*. We also included the Δ hopQ1-1 mutant of PtoDC3000 (PtoDC3000(Δ hQ)), which causes disease on *N. benthamiana* (Wei et al., 2007).

Unexpectedly, whilst the proteasome labeling upon infection with PtoDC3000(Δ hQ) is highly reproducible, we noticed that proteasome labeling upon infection with PtoDC3000(WT) differs significantly between eight independent infection assays. MVB072 labeling of extracts of PtoDC3000(WT)-infected leaves indicates that the activity of the proteasome is either upregulated (**Figure 6a**), or down regulated (**Figure 6b**). Importantly, labeling the same extracts with LW124+MVB127, provides much more insight. The lower $\beta 1$ signal either intensifies strongly upon PtoDC3000(WT) infection (**Figure 6c**, Supplemental **Figures S4-S5**), or only slightly (**Figure 6d**, Supplemental **Figures S6-S8**). Remarkably, however, the $\beta 5$ signal is either induced (**Figure 6c**, Supplemental **Figures S4-S5**) or strongly suppressed (**Figure 6d**, Supplemental **Figures S6-S8**). The fact that the ratio between $\beta 1$ and $\beta 5$ can differ between infection experiments significantly demonstrates that the activities of these two subunits can be uncoupled during bacterial infection. The cause of this phenotypic variation upon PtoDC3000(WT) infection is beyond the focus of the current manuscript, and is subject to further studies.

Proteasome activities upon infection by PtoDC3000(Δ hQ) show a robust 3-fold upregulation in the intensity of the $\beta 1$ and $\beta 5$ signals (**Figure 6e**, Supplemental **Figure S9**). Quantitative RT-PCR with gene-specific primers showed that also transcript levels of $\beta 1a$, $\beta 1b$ and $\beta 5$ are significantly upregulated (**Figure 6f**), indicating that the differential proteasome activity upon PtoDC3000(Δ hQ) is mostly transcriptional. Notably, we detect a highly reproducible shift in the ratio between the two $\beta 1$ signals upon infection with PtoDC3000(Δ hQ) (**Figure 6g**).

DISCUSSION

We have introduced next generation subunit-specific probes for labeling the $\beta 1$ and $\beta 5$ proteasome catalytic subunits, and validated labeling in both *Arabidopsis thaliana* and *Nicotiana benthamiana*. We also introduced and validated subunit-selective inhibitors for the $\beta 1$ and $\beta 5$ subunits, which may be useful for chemical knockout assays. We discovered that the active *N. benthamiana* proteasome contains different paralogous catalytic subunits: two for $\beta 1$, two for $\beta 2$ and two for $\beta 5$. Application of selective subunit labeling revealed and uncoupled induction in $\beta 1$ and $\beta 5$ subunits upon infection with virulent and avirulent *Pseudomonas syringae*.

Our data demonstrate that LW124 targets $\beta 1$ and MVB127 targets $\beta 5$. Because the proteasome subunits of *Arabidopsis* have a distinct MW, we would have detected additional signals if LW124 and MVB127 would label additional catalytic subunits. Likewise, MVB127 should have caused an additional signal if it could label $\beta 1$ of *N. benthamiana*. The absence of additional signals in *Arabidopsis* testifies the high selectivity of the subunit-selective probes.

By contrast, however, despite their structural similarity with the probes, the subunit-selective inhibitors partially suppress reciprocal labeling: N3 $\beta 1$ suppresses labeling of $\beta 5$ by MVB127 and N3 $\beta 5$ suppresses labeling by LW124, in both *Arabidopsis* (**Figure 2b**) and *N. benthamiana* (**Figure 4b**). Likewise, we detect a consistent suppression of $\beta 5$ labeling by MVB127 upon colabeling with LW124 (**Figures 1c, 2b, 4a and 4b**). Although we can not exclude at this stage that N3 $\beta 1$ and N3 $\beta 5$ are weak inhibitors of $\beta 5$ and $\beta 1$, respectively, the fact that the corresponding probes are subunit selective suggest an alternative explanation. The suppression of labeling by inhibitors and probes that target other subunits may also be caused by crowding of the proteolytic chamber (inhibitor bound to one subunit hinders access of probes to another subunit) or allosteric regulation (inhibition of one subunits affects labeling efficiency of another subunit). Although the proteolytic chamber is probably too large to support the crowded chamber hypothesis, the catalytic subunits of the proteasome are known to allosterically regulate each other, e.g. to facilitate the cyclical bite-chew mechanism (Kisselev et al., 1999).

N. benthamiana assembles different proteasomes

LW124 labeling of *N. benthamiana* displays two different $\beta 1$ signals. MS analysis of MVB072 labeled proteins confirmed that at least two different $\beta 1$ proteins are incorporated in proteasomes as active catalytic subunits. Subunits that are not incorporated into the proteasome remain in the inactive precursor state and are probably degraded (Chen & Hochstrasser, 1996). MS analysis of MVB072-labeled proteins also revealed at least two different $\beta 2$ proteins and two different $\beta 5$ subunits that must have been part of an active proteasome. However, MVB127 labeling only displays one $\beta 5$ signal, indicating that the labeled proteins run at the same height. The fact that multiple paralogs were identified demonstrates that *N. benthamiana* produces diverse catalytic subunits and might assemble different proteasomes.

The concept that plants can assemble multiple proteasomes is supported by the finding that Arabidopsis also incorporates paralogous subunits into the 26S proteasome (Yang et al., 2004; Book et al., 2010). Remarkably, little is known about the role of paralogous CP subunits but more about paralogous RP subunits. Different paralogs of a subunit may act redundantly. For example, the RPN1 subunit in Arabidopsis is encoded by two genes, *RPN1a* and *RPN1b*, which differ in their expression pattern (Yang et al., 2004). Nevertheless, *rpn1a* mutant lines maintain a functional proteasome indicating a redundant function (Wang et al., 2009). RPT2 and RPT5 isoforms also share redundant functions (Lee et al., 2011). In both Arabidopsis and maize, RPT2 and RPT5 are encoded by the paralogous genes *RPT2a* - *RPT2b* and *RPT5a* - *RPT5b*, respectively (Book et al., 2010). However, there are cases where paralogous subunits seem to have different functions. For example, *RPT5b* complements *RPT5a* in the *Col* ecotype, but not in *Ws* ecotype (Gallois et al., 2009), demonstrating an ecotype-dependent redundancy but also indicating alternative functions for the different isoforms. *N. benthamiana* is an allotetraploid, and the ancient genome duplication may explain a duplication of the proteasome subunits genes. At this stage, it is unclear if the different paralogous proteins have different functions.

Modification of the proteasome upon bacterial infection.

Interestingly, subunit-selective proteasome activity profiling revealed that the activity of the catalytic $\beta 5$ subunit can be strongly induced or suppressed upon infection with *Pseudomonas syringae* and show that the activities of $\beta 1$ and $\beta 5$ can be uncoupled during infection. Uncoupling is not expected for proteasome complexes that incorporate equal numbers of catalytic subunits, but may have been caused by selective subunit inhibition during infection with *P. syringae*, or the specific activation of the $\beta 1$ subunit during NHR/ETI responses.

Mammals have inducible subunits that can replace other β subunits, e.g. to create the immunoproteasome (Aki et al., 1994). Immunoproteasomes exhibit modified peptidase activities and variable cleavage site preferences. Their main function is the maintenance of cell homeostasis and cell viability under oxidative conditions (Seifert et al., 2010). It is likely that plants also possess a type of inducible proteasome where some catalytic subunits are replaced under biotic or abiotic stresses. We have identified six genes encoding $\beta 1$ catalytic subunits from the *N. benthamiana* genome, suggesting that the other isoforms that we did not detect by MS analysis are either expressed under different conditions, are tissue specific or are pseudogenes. This can also be the case for non identified $\beta 2$ and $\beta 5$ proteins. Induction of genes encoding α and β proteasome subunits has been described for tobacco cells treated with cryptogein (Dahan et al., 2001), whereas our earlier study revealed a post-translational upregulation of proteasome labeling upon treatment of Arabidopsis with benzodiazole (Gu et al., 2010). Transcript activation of proteasome genes after cryptogein treatment could be associated with oxidative stress, since attenuation of the oxidative burst blocks the expression of *$\beta 1din$* , *$\alpha 3din$* and *$\alpha 6din$* genes (Suty et al., 2003).

Thus, different paralogous proteasome subunits might be assembled in active proteasomes under different conditions, for instance responding to oxidative stress. The encoded catalytic subunits in *N. benthamiana* carry only few polymorphic amino acid residues, and it is unknown at this stage to what extent they affect proteasome function, e.g. with respect to substrate selection and conversion. This study uncovers that more research is needed to investigate the occurrence and function of alternative proteasomes in plants.

Taken together, we have introduced subunit-specific probes to monitor the $\beta 1$ and $\beta 5$ subunits of the plant proteasome. The use of site-specific probes combined with phylogenetic and proteomic analysis revealed multiple isoforms for the β subunits, indicating that different proteasomes co-exist in leaves. The subunit selective probes revealed unexpected, uncoupled differential activities of $\beta 1$ and $\beta 5$ upon bacterial infection, that raise exciting questions on the underlying mechanism and biological role in immunity.

EXPERIMENTAL PROCEDURES

Probes and inhibitors

The synthesis of LW124, MVB127, N3 $\beta 1$ and N3 $\beta 5$ has been described previously (Verdoes et al., 2010; Li et al., 2013). As with our previously introduced probes, aliquots of these chemicals are available upon request and frequent use may accelerate their commercial availability.

Plant material and labeling conditions

Arabidopsis thaliana ecotype Col-0 and *Nicotiana benthamiana* plants were grown in the greenhouse under a regime of 14 h light at 20 °C. 3–5 weeks old plants were used for labeling experiments. For *in vitro* labeling, leaves were ground in water containing 10 mM DTT and extracts were cleared by centrifugation. Labeling was performed by incubating the protein extract in 60 μ l buffer containing 66.7 mM Tris pH 7.5 and 0.5 – 0.8 μ M probe for 2 h at room temperature (22–25 °C) in the dark. After acetone precipitation pellets were re-suspended in 40 μ l 1x loading buffer and samples were separated on 12% SDS gel. Inhibitory assays were performed by 30 min pre-incubation of protein extracts with 50 μ M of the inhibitor of interest, followed by 2 h labeling. For *in vivo* inhibition of the proteasome 50 μ M of the inhibitor was infiltrated in *N. benthamiana* leaves using a syringe without a needle. After 6 h incubation at room temperature, a leaf disc (1.6 cm diameter) of the infiltrated area was collected and labeled with the probe of interest as described above. Labeled proteins were visualized by in-gel fluorescence scanning using a Typhoon FLA 9000 scanner (GE Healthcare, <http://www.gelifesciences.com>) with Ex473/Em530 nm for LW124 and Ex532/Em580 nm for MVB127, MVB072 and RhSylA. Fluorescent signals were quantified using ImageQuant 5.2 (GE Healthcare) with the rolling ball method for background correction. To confirm equal loading, Coomassie brilliant blue or SyproRuby (Invitrogen) staining was performed according to the

instructions of the manufacturer. SyproRuby gels were fluorescent scanned (Ex472/Em580 nm) and used for loading correction in the quantification of fluorescent signals. Statistical significance was calculated with a student's t-test of at least three replicates.

Large scale pull down assay

Large scale pull down experiments were performed once on plants treated with benzothiadiazole (BTH) and once on the water control. This material was generated by spraying 3-4-week old *N. benthamiana* plants with 0.13 mg/mL BTH (BION, Syngenta) containing 0.01% Silwet L-77 (Lehle Seeds) or sprayed with water containing the same concentration of Silwet L-77. Leaves were harvested two days after treatment. 44 leaf discs of 2.3 cm diameter were collected per sample and ground in a buffer containing 1 mM DTT and 67 mM Tris pH 7.5. After centrifugation, 10 ml of protein extract was used for labeling with 20 μ M MVB072 or 2.5 μ l DMSO. Samples were incubated at room temperature and in the dark with gentle shaking for 2 h. Labeling was stopped by precipitating total proteins via the chloroform/methanol precipitation method (Wessel and Flügge, 1984). Affinity purification and in-gel digestion was performed as described elsewhere (Chandrasekar et al., 2014).

Mass spectrometry

LC-MS/MS Experiments were performed on an Orbitrap Elite instrument (Thermo, Michalski et al. 2012) that was coupled to an EASY-nLC 1000 liquid chromatography (LC) system (Thermo). The LC was operated in the one-column mode. The analytical column was a fused silica capillary (75 μ m \times 15 cm) with an integrated PicoFrit emitter (New Objective) packed in-house with Reprosil-Pur 120 C18-AQ 1.9 μ m resin (Dr. Maisch). The LC was equipped with two mobile phases: solvent A (0.1% formic acid, FA, in water) and solvent B (0.1% FA in acetonitrile, ACN). All solvents were of UPLC grade (Sigma). Peptides were directly loaded onto the analytical column with a maximum flow rate that would not exceed the set pressure limit of 800 bar (usually around 0.7 – 0.8 μ l/min). Peptides were subsequently separated on the analytical column by running a 60 min or 120 min gradient of solvent A and solvent B (60 min runs: start with 2% B; gradient 2% to 10% B for 2.5 min; gradient 10% to 35% B for 45 min; gradient 35% to 45% B for 7.5 min; gradient 45% to 100% B for 2 min and 100% B for 3 min. 120 min runs: start with 2% B; gradient 2% to 10% B for 5 min; gradient 10% to 35% B for 90 min; gradient 35% to 45% B for 15 min; gradient 45% to 100% B for 4 min and 100% B for 6 min.) at a flow rate of 300 nl/min. The mass spectrometer was operated using Xcalibur software (version 2.2 SP1.48). The mass spectrometer was set in the positive ion mode. Precursor ion scanning was performed in the Orbitrap analyzer (FTMS) in the scan range of m/z 300-1800 and at a resolution of 60000 with the internal lock mass option turned on (lock mass was 445.120025 m/z , polysiloxane) (Olsen et al., 2005). Product ion spectra were recorded in a data dependent fashion in the ion trap (ITMS) in a variable scan range and at a rapid scan rate. The ionization potential (spray voltage) was set to 1.8 kV. Peptides were analyzed using a repeating cycle consisting of a full precursor ion scan

(1.0×10^6 ions or 200 ms) followed by 15 product ion scans (1.0×10^4 ions or 50 ms) where peptides are isolated based on their intensity in the full survey scan (threshold of 500 counts) for tandem mass spectrum (MS2) generation that permits peptide sequencing and identification. CID collision energy was set to 35% for the generation of MS2 spectra. For the 2 h gradient length the data dependent decision tree option and supplemental activation was switched on. The ETD reaction time was 100 ms. During MS2 data acquisition dynamic ion exclusion was set to 30 seconds with a maximum list of excluded ions consisting of 500 members and a repeat count of one. Ion injection, time prediction, preview mode for the FTMS, monoisotopic precursor selection and charge state screening were enabled. Only charge states higher than 1 were considered for fragmentation.

Peptide and Protein Identification using MaxQuant

RAW spectra were submitted to an Andromeda (Cox et al., 2011) search in MaxQuant (version 1.5.3.30) using the default settings (Cox et al., 2008) Match-between-runs was activated (Cox et al., 2014) MS/MS spectra data were searched against the in-house generated *Nicotiana benthamiana* database (78729 entries). All searches included a contaminants database (as implemented in MaxQuant, 267 sequences). The contaminants database contains known MS contaminants and was included to estimate the level of contamination. Andromeda searches allowed oxidation of methionine residues (16 Da) and acetylation of protein N-terminus (42 Da) as dynamic modification and the static modification of cysteine (57 Da, alkylation with iodoacetamide). Enzyme specificity was set to “Trypsin/P”. The instrument type in Andromeda searches was set to Orbitrap and the precursor mass tolerance was set to ± 20 ppm (first search) and ± 4.5 ppm (main search). The MS/MS match tolerance was set to ± 0.5 Da. The peptide spectrum match FDR and the protein FDR were set to 0.01 (based on target-decoy approach). Minimum peptide length was 7 amino acids. The minimum score for modified peptides was 40.

Extraction of proteasome specific peptides

The peptide.txt output files from MaxQuant were loaded into Perseus v1.5.3.0. After removal of peptides matching to the reversed database and peptides matching to the contaminant database the remaining peptides were annotated using an in-house annotation file (annotation.wOG.txt). Peptides annotated to be derived from the proteasome or a proteasome subunit were extracted (Supplementary **Table S1**) and manually mapped to the individual proteasome sequences (Supplementary **Figure S2**).

Database search and phylogenetic analysis

The *N. benthamiana* database (v. 0.4.4, 76,379 sequences) was downloaded from the SOL genomics network (<https://solgenomics.net>) and a blast search using Arabidopsis catalytic subunits as a template was performed. Additionally, *N. benthamiana* annotated T1 proteins found in the MEROPS database (<https://merops.sanger.ac.uk>) were compared with the hits obtained by the search with Arabidopsis

orthologs. The sequences were aligned with ClustalX2 (Larkin et al., 2007) standalone program. The alignment parameters were used as follows: the pair wise alignment gap opening penalty 30 and gap extension penalty 0.75, whereas for multiple alignment gap opening penalty were set to 15 and gap extension penalty to 0.3. Finally, the output alignment file from the ClustalX2 was used to generate the tree in R (Charif and Lobry, 2007; Paradis et al., 2004). The neighbor-joining algorithm was implemented in the script for the construction of the phylogenetic tree from the calculated distance matrix.

Bacterial infections

For *P. syringae* infection, leaves of five-week old *N. benthamiana* plants were infiltrated using a needle-less syringe with 10^6 CFU/mL *Pseudomonas syringae* pv. *tomato* DC3000 and its $\Delta hopQ1-1$ mutant derivative (Wei et al., 2007). Three leaf discs (d=1 cm) were harvested at days 1 and 2. Leaf extracts were generated in 200 μ L of 50 mM Tris buffer at pH 7.5 containing 5 mM DTT, cleared by centrifugation and labeled for two hours with 0.2 μ M MVB072 or 0.8 μ M LW124 + 0.8 μ M MVB127 at room temperature in the dark in 50 μ L total volume.

Nucleic acid preparation, cDNA synthesis and qRT-PCR

For RNA extraction, leaf material of *N. benthamiana* infected leaves was frozen in liquid nitrogen, ground to powder. The RNA was extracted using Trizol (Ambion), treated with DNase (QIAGEN), purified using the RNeasy Plant Mini Kit (QIAGEN) and used the SuperScriptTM III Reverse Transcriptase (Invitrogen) for cDNA synthesis. The first-strand cDNA synthesis kit was used to reverse transcribe 1 μ g of total RNA with oligo(dT) Primers. The qRT-PCR analysis was performed using the iQ SYBR Green Supermix (Bio-Rad) with an iCycler (Bio-Rad). Specific primers were used to amplify $\beta 1a$ (forward: 5'-ctgctggatattgtgcctgc-3', reverse: 5'-ggctcaaacatgctgacagt-3'), $\beta 1b$ (forward: 5'-tgcccctattcacgtgttg-3', reverse: 5'-gttgacagcaggacaaaagga-3'), $\beta 5b$ (forward: 5'-ctcccattctacgtgcgtca-3', reverse: 5'-ggattgacttgcttagctcac-3') and *PP2A* (forward: 5'-gacctgatgttgatgttcgct-3', reverse: 5'-gagggattgaagagagatttc-3') was used as reference gene for normalization. Cycling conditions were as follows: 3 min at 95°C, followed by 45 cycles of 15 sec at 95°C, 15 sec at 60°C and 30 sec at 72°C. After each PCR, the specificity of the amplified product was verified with the melting curves. Gene expression levels for $\beta 1a$, $\beta 1b$ and $\beta 5a$ were then calculated relative to *PP2A* using the $2^{-\Delta Ct}$ (cycle threshold) method (Livak and Schmittgen, 2001). The average expression and the standard deviation of one experiment with four individuals were calculated, and expression of the mock control was set to 1. P values were calculated using a two tails *t*-test with unequal variance. P values <0.0005 were marked with three asterisks.

ACKNOWLEDGEMENTS

516 We would like to thank Prof. Gunther Doehleman and Prof. George Coupland for their support. We
517 are grateful to Prof. Collmer for providing the Δ hopQ1-1 mutant of PtoDC3000. This work was
518 financially supported by the Max Planck Society, ERC Consolidator grant (R.H., grant No. 616449
519 ‘GreenProteases’), an ERC starting grant (M.K., grant No. 258413), the Deutsche
520 Forschungsgemeinschaft (M.K., grant no. INST 20876/127-1 FUGG) and the University of Oxford.

REFERENCES

- Aki, M., Shimbara, N., Takashina, M., Akiyama, K., Kagawa, S., Tamura, T., Tanahashi, N., Yoshimura, T., Tanaka, K. and Ichihara, A.** (1994) Interferon-gamma induces different subunit organizations and functional diversity of proteasomes. *J. Biochem.* **115**, 257-269.
- Banfield, M.J.** (2015) Perturbation of host ubiquitin systems by plant pathogen/pest effector proteins. *Cell Microbiol.* **17**, 18-25.
- Book, A.J., Gladman, N.P., Lee, S.S., Scalf, M., Smith, L.M. and Vierstra, R.D.** (2010) Affinity purification of the Arabidopsis 26S proteasome reveals a diverse array of plant proteolytic complexes. *J. Biol. Chem.* **285**, 25554–25569.
- Carrión, C.A., Costa, M.L., Martínez, D.E., Mohr, C., Humbeck, K. and Guamet, J.J.** (2013) *In vivo* inhibition of cysteine proteases provides evidence for the involvement of 'senescence-associated vacuoles' in chloroplast protein degradation during dark-induced senescence of tobacco leaves. *J. Exp. Bot.* **64**, 4967-4980.
- Chandrasekar, B., Colby, T., Emon, A.E.K., Jiang, J., Hong, T.N., Villamor, J.G., Harzen, A., Overkleeft, H.S. and Van der Hoorn, R.A.L.** (2014) Broad range glycosidase activity profiling. *Mol. Cell. Proteomics* **13**, 2787-2800.
- Charif, D. and Lobry, J.** (2007) SeqinR 1.0–2: a contributed package to the R project for statistical computing devoted to biological sequences retrieval and analysis. In: Structural Approaches to Sequence Evolution (Bastolla U., Porto M., Roman H. E., Vendruscolo M., eds), pp. 207–232, Springer, Berlin
- Chen, P. and Hochstrasser, M.** (1996) Autocatalytic subunit processing couples active site formation in the 20S proteasome to completion of assembly. *Cell* **86**, 961–972.
- Cox, J., Hein, M.Y., Lubner, C.A., Paron, I., Nagaraj, N. and Mann, M.** (2014) Accurate Proteome-wide Label-free Quantification by Delayed Normalization and Maximal Peptide Ratio Extraction, Termed MaxLFQ. *Mol. Cell. Proteomics* **13**, 2513-2526.
- Cox, J. and Mann, M.** (2008) MaxQuant enables high peptide identification rates, individualized p.p.b.-range mass accuracies and proteome-wide protein quantification. *Nat. Biotechnol* **26**, 1367-1372.
- Cox, J., Neuhauser, N., Michalski, A., Scheltema, R.A., Olsen, J.V. and Mann, M.** (2011) Andromeda: a peptide search engine integrated into the MaxQuant environment. *J. Proteome Res.* **10**, 1794-1805.
- Cravatt, B.F., Wright, A.T. and Kozarich, J.W.** (2008) Activity-based protein profiling: from enzyme chemistry to proteomic chemistry. *Annu. Rev. Biochem.* **77**, 383–414.
- Dahan, J., Etienne, P., Petitot, A.S., Houot, V., Blein, J.P. and Suty, L.** (2001) Cryptogein affects expression of $\alpha 3f$, $\alpha 6$ and $\beta 1$ proteasome subunits encoding gene in tobacco. *J. Exp. Bot.* **52**, 1947-1948.

557 **Dick, T.P., Nussbaum, A.K., Deeg, M., Heinemeyer, W., Groll, M., Schirle, M., Keilholz, W.,**
558 **Stevanović, S., Wolf, D.H., Huber, R., Rammensee, H.G. and Schild, H.** (1998) Contribution of
559 proteasomal β -subunits to the cleavage of peptide substrates analyzed with yeast mutants. *J. Biol.*
560 *Chem.* **273**, 25637-25646.

561 **Dong, S., Stam, R., Cano, L.M., Song, J., Sklenar, J., Yoshida, K., Bozkurt, T.O., Oliva, R., Liu**
562 **,Z., Tian, M., Win, J., Banfield, M.J., Jones, A.M., Van der Hoorn, R.A.L. and Kamoun, S.**
563 (2014) Effector specialization in a lineage of the Irish potato famine pathogen. *Science* **343**, 552-555.

564 **Gallois, J.L., Guyon-Debast, A., Le´ cureuil, A., Vezon, D., Carpentier, V., Bonhomme, S. and**
565 **Guerche, P.** (2009) The Arabidopsis proteasome RPT5 subunits are essential for gametophyte
566 development and show accession-dependent redundancy. *Plant Cell* **21**, 442-459.

567 **Goodin, M.M., Zaitlin, D., Naidu, R.A. and Lommel, S.A.** (2008) *Nicotiana benthamiana*: Its
568 history and future as a model for plant–pathogen interactions. *Mol. Plant-Microbe Interact.* **21**, 1015-
569 1026.

570 **Greenbaum, D., Medzihradszky, K.F., Burlingame, A. and Bogyo, M.** (2000) Epoxide
571 electrophiles as activity-dependent cysteine protease profiling and discovery tools. *Chem. Biol.* **7**, 569-
572 581.

573 **Groll, M., Ditzel, L., Löwe, J., Stock, D., Bochtler, M., Bartunik, H.D. and Huber, R.** (1997)
574 Structure of 20S proteasome from yeast at 2.4 Å resolution. *Nature* **386**, 463-471.

575 **Groll, M., Schellenberg, B., Bachmann, A.S., Archer, C.R., Huber, R., Powell, T.K., Lindow, S.,**
576 **Kaiser, M. and Dudler, R.** (2008) A plant pathogen virulence factor inhibits the eukaryotic
577 proteasome by a novel mechanism. *Nature* **452**, 755-758.

578 **Gu, C., Kolodziejek, I., Misas-Villamil, J.C., Shindo, T., Colby, T., Verdoes, M., Richau, K.H.,**
579 **Schmidt, J., Overkleef, H.S. and Van der Hoorn, R.A.L.** (2010) Proteasome activity profiling: a
580 simple, robust and versatile method revealing subunit-selective inhibitors and cytoplasmic, defence-
581 induced proteasome activities. *Plant J.* **62**, 160-170.

582 **Gu, C.** (2009) Activity-based protein profiling in plants. PhD Thesis, University of Cologne.

583 **Hörger, A.C., Ilyas, M., Stephan, W., Tellier, A., Van der Hoorn, R.A.L. and Rose, L.E.** (2012)
584 Balancing selection at the tomato RCR3 guard gene family maintains variation in strength of
585 pathogen defense. *PLoS Genetics* **8**, e1002813.

586 **Kaschani, F., Shabab, M., Bozkurt, T., Shindo, T., Schornack, S., Gu, C., Ilyas, M., Win, J.,**
587 **Kamoun, S. and Van der Hoorn, R.A.L.** (2010) An effector-targeted protease contributes to defense
588 against *Phytophthora infestans* and is under diversifying selection in natural hosts. *Plant Physiol.* **154**,
589 1794-1804.

590 **Kisselev, A. F., Kopian, T. N., Castillo, V., and Goldberg, A. L.** (1999) Proteasome active sites
591 allosterically regulate each other, suggesting a cyclical bite-chew mechanism for protein breakdown.
592 *Mol. Cell* **4**, 395-402.

593 **Kolodziejek, I., Misas-Villamil, J.C., Kaschani, F., Clerc, J., Gu, C., Krahn, D., Niessen, S.,**
594 **Verdoes, M., Willems, L.I., Overkleeft, H.S., Kaiser, M. and Van der Hoorn, R.A.L.** (2011)
595 Proteasome activity imaging and profiling characterizes bacterial effector Syringolin A. *Plant Physiol.*
596 **155**, 477-489.

597 **Kurepa, J. and Smalle, J.A.** (2008a) Structure, function and regulation of plant proteasomes.
598 *Biochimie* **90**, 324-335.

599 **Larkin, M.A., Blackshields, G., Brown, N.P., Chenna, R., McGettigan, P.A., McWilliam, H.,**
600 **Valentin, F., Wallace, I.M., Wilm, A., Lopez, R., Thompson, J.D., Gibson, T.J. and Higgins, D.G.**
601 (2007) Clustal W and Clustal X version 2.0. *Bioinformatics* **23**, 2947-2948.

602 **Lee, K.H., Minami, A., Marshall, R.S., Book, A.J., Farmer, L.M., Walker, J.M. and Vierstra,**
603 **R.D.** (2011) The RPT2 subunit of the 26S proteasome directs complex assembly, histone dynamics,
604 and gametophyte and sporophyte development in Arabidopsis. *Plant Cell* **23**, 4298-4317.

605 **Li, N., Kuo, C.L., Paniagua, G., van den Elst, H., Verdoes, M., Willems, L.I., Van der Linden,**
606 **W.A., Ruben, M., Van Genderen, E., Gubbens, J., Van Wezel, G.P., Overkleeft, H.S. and Florea,**
607 **B.I.** (2013) Relative quantification of proteasome activity by activity-based protein profiling and LC-
608 MS/MS. *Nat. Protocols* **8**, 1155-1168.

609 **Livak K.J. and Schmittgen, T.D.** (2001) Analysis of relative gene expression data using real-time
610 quantitative PCR and the 2(-Delta Delta C(T)) Method. *Methods*. **25**, 402-408.

611 **Martínez, D.E., Bartoli, C.G., Grbic, V. and Guamet, J.J.** (2007) Vacuolar cysteine proteases of
612 wheat (*Triticum aestivum* L.) are common to leaf senescence induced by different factors. *J. Exp. Bot.*
613 **58**, 1099-1107.

614 **Michalski, A., Damoc, E., Lange, O., Denisov, E., Nolting, D., Muller, M., Viner, R., Schwartz,**
615 **J., Belford, M., Dunyach, J.J., Cox, J., Horning, S., Mann, M. and Makarov, A.** (2012) Ultra high
616 resolution linear ion trap Orbitrap mass spectrometer (Orbitrap Elite) facilitates top down LC MS/MS
617 and versatile peptide fragmentation modes. *Mol. Cell. Proteomics* **11**, O111.013698.

618 **Misas-Villamil, J.C., Kolodziejek, I., Crabill, E., Kaschani, F., Niessen, S., Shindo, T., Kaiser,**
619 **M., Alfano, J.R. and Van der Hoorn, R.A.L.** (2013) *Pseudomonas syringae* pv. *syringae* uses
620 proteasome inhibitor Syringolin A to colonize from wound infection sites. *PLoS Pathogens* **9**,
621 e1003281.

622 **Morimoto, K. and Van der Hoorn, R.A.L.** (2016) The increasing impact of activity-based protein
623 profiling in plant science. *Plant Cell Physiol.* **57**, 446-461.

624 **Mueller, A.N., Ziemann, S., Treitschke, S., Aßmann, D. and Doehlemann, G.** (2013)
625 Compatibility in the *Ustilago maydis*-maize interaction requires inhibition of host cysteine proteases
626 by the fungal effector Pit2. *PLoS Pathog.* **9**, e1003177.

627 **Nguyen, H. M., Schippers, J. H., Goni-Ramos, O., Christoph, M. P., Dortay, H., Van der Hoorn,**
628 **R. A. L., and Mueller-Roeber, B.** (2013) An upstream regulator of the 26S proteasome modulates
629 organ size in *Arabidopsis thaliana*. *Plant J.* **74**, 25-36.

630 **Olsen, J.V., de Godoy, L.M., Li, G., Macek, B., Mortensen, P., Pesch, R., Makarov, A., Lange,**
631 **O., Horning, S. and Mann, M.** (2005) Parts per million mass accuracy on an Orbitrap mass
632 spectrometer via lock mass injection into a C-trap. *Mol. Cell. Proteomics* **4**, 2010-2021.

633 **Padmanabhan, A., Vuong, S.A. and Hochstrasser, M.** (2016) Assembly of an evolutionary
634 conserved alternative proteasome isoform in human cells. *Cell Rep.* **14**, 2962-2974.

635 **Paradis, E., Claude, J. and Strimmer, K.** (2004) APE: analyses of phylogenetics and evolution in R
636 language. *Bioinformatics* **20**, 289-290.

637 **Poret, M., Chandrasekar, B., Van der Hoorn, R.A.L. and Avice, J.B.** (2016) Characterization of
638 senescence-associated protease activities in the efficient protein remobilization during leaf senescence
639 of winter oilseed rape. *Plant Sci.* **246**, 139-153.

640 **Rooney, H., Van 't Klooster, J., Van der Hoorn, R.A.L., Joosten, M.H.A.J., Jones, J.D.G. and De**
641 **Wit, P.J.G.M.** (2005) Cladosporium Avr2 inhibits tomato Rcr3 protease required for Cf-2-dependent
642 disease resistance. *Science* **308**, 1783-1789.

643 **Schellenberg B., Ramel, C. and Dudler, R.** (2010) *Pseudomonas syringae* virulence factor
644 Syringolin A counteracts stomatal immunity by proteasome inhibition. *Mol. Plant-Microbe Interact.*
645 **23**, 1287-1293.

646 **Seifert, U., Bialy, L.P., Ebstein, F., Bech-Otschir, D., Voigt, A., Schröter, F., Prozorovski, T.,**
647 **Lange, N., Steffen, J., Rieger, M., Kuckelkorn, U., Aktas, O., Kloetzel, P.M. and Krüger, E.**
648 (2010) Immuno-proteasomes preserve protein homeostasis upon interferon-induced oxidative stress.
649 *Cell* **142**, 613-624.

650 **Shabab, M., Shindo, T., Gu, C., Kaschani, F., Pansuriya, T., Chintla, R., Harzen, A., Colby, T.,**
651 **Kamoun, S. and Van der Hoorn, R.A.L.** (2008) Fungal effector protein AVR2 targets diversifying
652 defence-related Cys proteases of tomato. *Plant Cell* **20**, 1169-1183.

653 **Song, J., Win, J., Tian, M., Schornack, S., Kaschani, F., Muhammad, I., Van der Hoorn, RAL.**
654 **and Kamoun, S.** (2009) Apoplastic effectors secreted by two unrelated eukaryotic plant pathogens
655 target the tomato defense protease Rcr3. *Proc. Natl. Acad. Sci. USA* **106**, 1654-1659.

656 **Suty, L., Lequeu, J., Lancon, A., Etienne, P., Petitot, A.S. and Blein, J.P.** (2003) Preferential
657 induction of 20S proteasome subunits during elicitation of plant defense reactions: towards the
658 characterization of plant defense proteasomes. *Int. J. Biochem. Cell. Biol.* **35**, 637-650.

659 **Tian, M., Win, J., Song, J., Van der Hoorn, R.A.L., Van der Knaap, E. and Kamoun, S.** (2007) A
660 *Phytophthora infestans* cystatin-like protein interacts with and inhibits a tomato papain-like apoplastic
661 protease. *Plant Physiol.* **143**, 364-277.

662 **Üstün, S., Bartetzo, V. and Bornke, F.** (2013) The *Xanthomonas campestris* type III effector XopJ
663 targets the host cell proteasome to suppress salicylic-acid mediated plant defence. *PLoS Pathog.* **9**,
664 e1003427.

665 **Üstün, S., König, P., Guttman, D.S. and Bornke, F.** (2014) HopZ4 from *Pseudomonas syringae*, a
 666 member of the HopZ type III effector family from the YopJ superfamily, inhibits the proteasome in
 667 plants. *Mol. Plant-Microbe Interact.* **27**, 611-623.
 668 **Üstün S, Sheikh A, Gimenez-Ibanez S, Jones A, Ntoukakis V, Börnke F.** (2016) The proteasome
 669 acts as a hub for plant immunity and is targeted by *Pseudomonas* type III effectors. *Plant Physiol.* **172**,
 670 1941-1958.
 671 **Van der Hoorn, R.A.L., Leeuwenburgh, M.A., Bogyo, M., Joosten, M.H.A.J. and Peck, S.C.**
 672 (2004) Activity profiling of papain-like cysteine proteases in plants. *Plant Physiol.* **135**, 1170-1178.
 673 **Van Esse, H.P., Van't Klooster, J.W., Bolton, M.D., Yadeta, K.A., Van Baarlen, P, Boeren, S.,**
 674 **Vervoort, J., De Wit, P.J.G.M. and Thomma, B.P.H.J.** (2008) The *Cladosporium fulvum* virulence
 675 protein Avr2 inhibits host proteases required for basal defense. *Plant Cell* **20**, 1948-1963.
 676 **Verdoes, M., Willems, L.I., Van der Linden, W.A., Duivenvoorden, B.A., Van der Marel, G.A.,**
 677 **Florea, B.I., Kisselev, A.F. and Overkleeft, H.S.** (2010) A panel of subunit-selective activity-based
 678 proteasome probes. *Org. Biomol. Chem.* **8**, 2719-2727.
 679 **Wang, S., Kurepa, J. and Smalle, J.A.** (2009) The Arabidopsis 26S proteasome subunit RPN1a is
 680 required for optimal plant growth and stress responses. *Plant Cell Physiol.* **50**, 1721-1725.
 681 **Wei, C.F., Kvitko, B.H., Shimizu, R., Crabill, E., Alfano, J.R., Lin, N.C., Martin, G.B., Huang,**
 682 **H.C. and Collmer, A.** (2007) A *Pseudomonas syringae* pv. *tomato* DC3000 mutant lacking the type
 683 III effector HopQ1-1 is able to cause disease in the model plant *Nicotiana benthamiana*. *Plant J.* **51**,
 684 32-46.
 685 **Wessel, D. and Flügge, U.I.** (1984) A method for the quantitative recovery of protein in dilute-
 686 solution in the presence of detergents and lipids. *Anal. Biochem.* **138**, 141-143.
 687 **Yang, P., Fu, H., Walker, J.M., Papa, C.M., Smalle, J.A., Ju, Y.M. and Vierstra, R.D.** (2004)
 688 Purification of the Arabidopsis 26S proteasome: biochemical and molecular analyses revealed the
 689 presence of multiple isoforms. *J. Biol. Chem.* **279**, 6401-6413.
 690

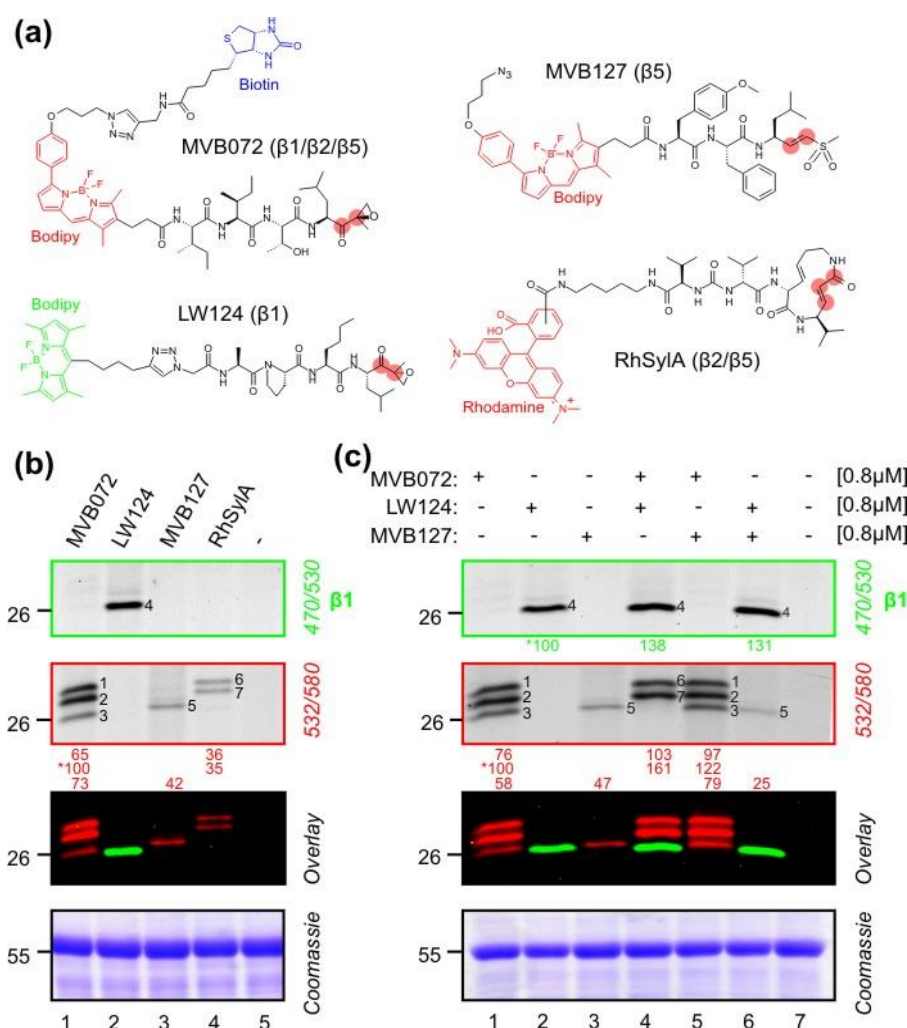


Figure 1. Subunit-specific labeling of Arabidopsis proteasome catalytic subunits

(a) Structures of probes used in this study. MVB072 carries an epoxyketone reactive group, a Ile-Ile-Ser-Leu tetrapeptide mimic and both a Bodipy TAMRA fluorophore (ex532/em580, red) and a biotin affinity handle. LW124 contains an epoxyketone reactive group on a Ala-Pro-Nle-Leu tetrapeptide mimic, and a Bodipy Cy2 fluorophore (ex470/em530, green). MVB127 carries a vinyl sulfone (VS) reactive group, a MeTyr-Phe-Ile tripeptide and both an azide minitag and a Bodipy TAMRA fluorophore (ex532/em580, red). RhSylA contains a Michael system reactive group embedded in a syringolin A (SylA) structure and carries a Rhodamine fluorophore (ex532/em580, red). Sites that are targeted by the catalytic Thr of the proteasome are highlighted with red circles.

(b) Comparison of the different labeling profiles generated with the four different probes. Arabidopsis leaf extracts were labeled at pH 7.5 with 0.8 μM MVB072, LW124 and MVB127 for 2 h and with 0.5 μM RhSylA for 30 min. Fluorescent proteins were detected by in-gel fluorescent scanning at two indicated settings. Numbers on the gel annotate signals caused by the labeled proteins. Numbers below the gel show the intensity of the fluorescent signals, as a percentage compared to the reference signal indicated by an asterisk. See Figure S1 for entire gels. This experiment was performed at least three independent times with similar results.

708 (c) (Co)labeling of proteasome subunits with the different probes. Arabidopsis leaf extracts were
709 (co)labeled with MVB072, LW124, MVB127 for 2 h. Fluorescent proteins were detected as described
710 in (b). This experiment has been reproduced at least three independent times with similar results.
711

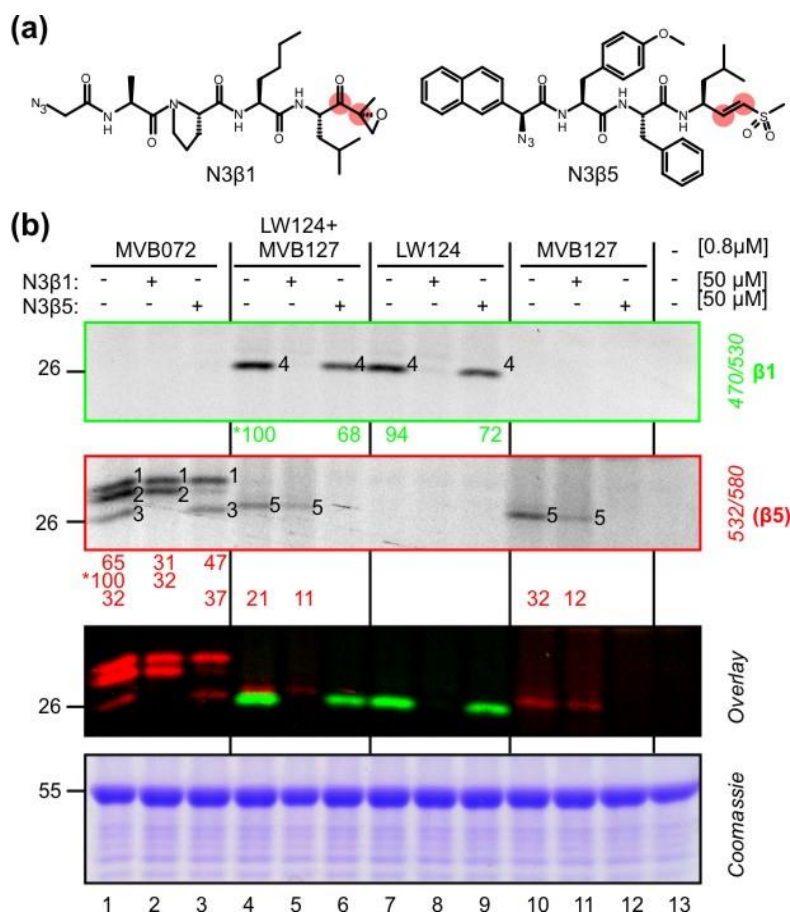


Figure 2. Subunit-selective inhibitors confirm selective subunit labeling

(a) Structures of specific inhibitors for the β 1 and β 5 proteasome catalytic subunits. N3 β 1 is an epoxyketone specific inhibitor of the β 1 catalytic subunit of the proteasome. N3 β 5 is a vinyl sulphone based inhibitor that specifically targets the β 5 catalytic subunit of the proteasome. Both inhibitors contain an azide group. Reactive groups are indicated with red circles.

(b) Subunit-specific inhibitors confirm subunit-selective labeling by LW124 and MVB127.

Arabidopsis leaf extracts were pre-incubated with 50 μ M N3 β 1 or N3 β 5 for 30 min, followed by (co)labeling with MVB072, LW124 and MVB127 for 2 h. Fluorescent proteins were detected and annotated with numbers as described in **Figure 1b**. The experiment has been reproduced at least three independent times with similar results.

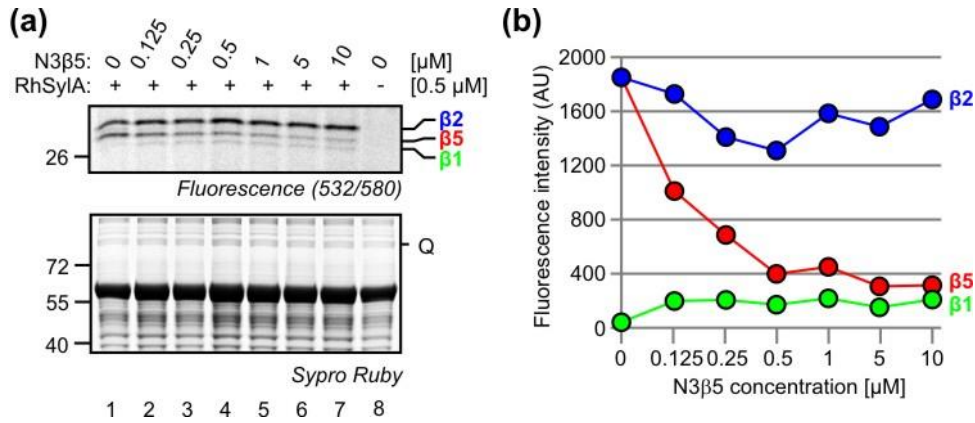


Figure 3. Selective β2 labeling using [RhSylA + N3β5]

(a) In the presence of N3β5, RhSylA labels β2 selectively. Arabidopsis leaf extracts were pre-incubated with increasing concentrations of the β5 selective inhibitor N3β5 for 15 min followed by labeling with 0.5 μM RhSylA for 30 min. Proteins were detected by in-gel fluorescent scanning and Sypro Ruby staining. This experiment has been repeated four independent times with similar results.

(b) Quantification of fluorescence labeling. Fluorescent signals corresponding to the catalytic subunits β1, β2 and β5 were quantified from fluorescent gels. Fluorescence intensity values were normalized for loading using the Sypro Ruby signal Q, indicated in (a). Values for the catalytic subunits were plotted against different N3β5 concentrations. A reproduction of this experiment is shown as Figure S3.

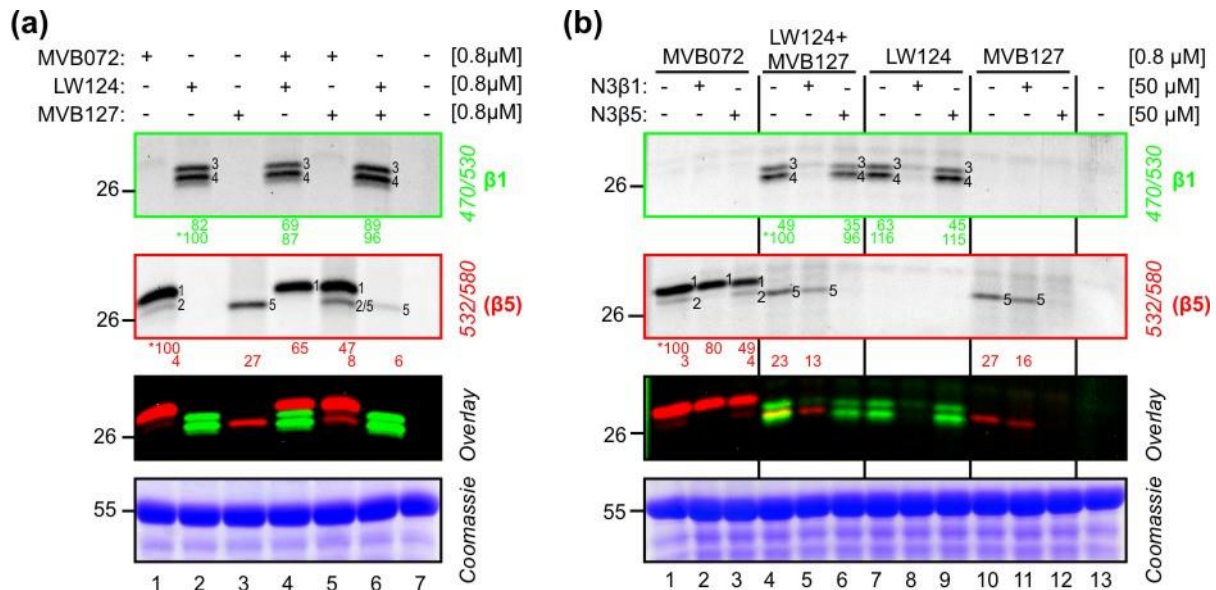


Figure 4. Labeling of *N. benthamiana* proteasome with subunit-specific probes

(a) Labeling profiling of proteasome specific probes. *N. benthamiana* leaves extracts were (co)labeled at pH 7.5 with 0.8 μM MVB072, LW124 and MVB127 for 2 h. Fluorescent proteins were detected as described in **Figure 1b**. Numbers on gels annotate the different signals caused by labeled proteasome subunits. This experiment has been reproduced at least three independent times with similar results.

(b) Selective (co)labeling of β1 and β5 of *N. benthamiana*. *N. benthamiana* extracts were pre-incubated with 50 μM of the selective proteasome inhibitors N3β1 and N3β5 for 30 min followed by 2 h (co)labeling with 0.8 μM MVB072, LW124 and MVB127. Fluorescent proteins were detected as described in **Figure 1b**. Shown is a representative gel of three independent biological replicates.

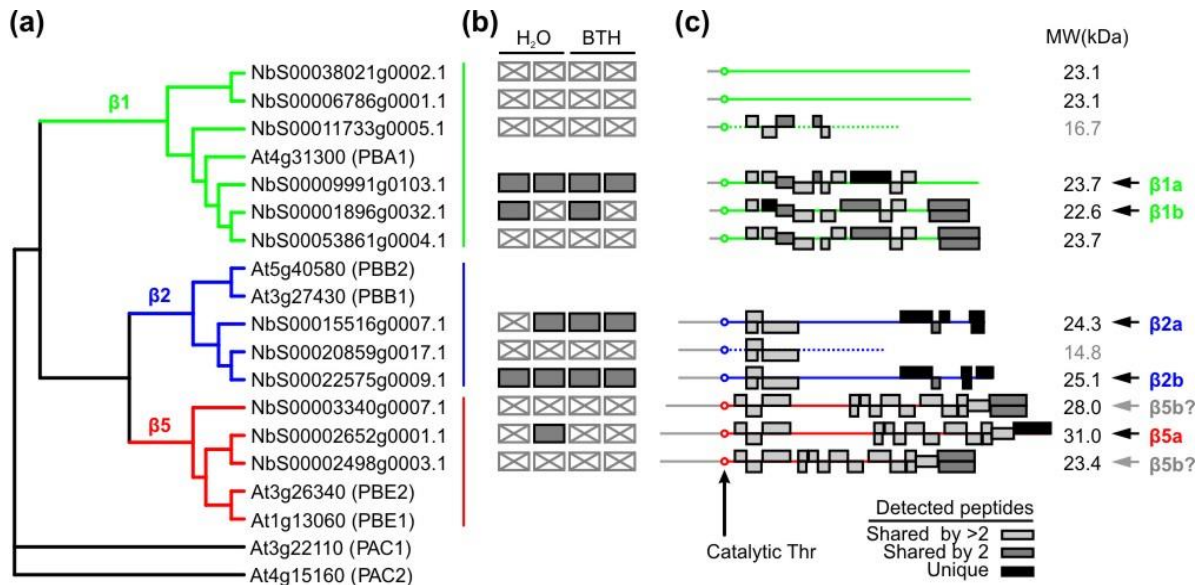


Figure 5. Detection of the expanded proteasome subunit repertoire of *N. benthamiana*

(a) Neighbour-joining phylogenetic tree of $\beta 1$, $\beta 2$, and $\beta 5$ catalytic subunits of the proteasome of Arabidopsis and *N. benthamiana*, rooted with the $\alpha 3$ subunit (PAC1 and PAC2).

(b) Identification of unique peptides upon MVB072 pull down from *N. benthamiana* leaf extracts. Leaf extracts from plants treated with water or BTH were labeled with MVB072 and the labeled proteins purified on avidin beads, eluted and separated on protein gels. Proteins were digested in-gel with trypsin and the eluted peptides were analyzed twice by mass spectrometry. Filled grey boxes indicate the detection of unique peptides of the respective proteasome subunit, whereas crossed boxes indicate no unique peptides detected.

(c) Position of detected peptides of the catalytic subunits. Shown are the peptides that are unique (black); shared with one other subunit (dark grey); or shared with more than one subunit (light grey). Grey lines indicate the propeptide that is removed upon proteasome assembly. The mature protein starts with a catalytic Thr residue. Truncated $\beta 1$ and $\beta 2$ proteasome subunits that may not be functional are shown as dashed lines. The molecular weight (MW) indicates the calculated MW of the mature subunit (without propeptide) in kilo Dalton (kDa). Black arrows indicate subunits that were identified with unique peptide(s), and the grey arrow indicates the identified $\beta 5$ subunit, in case the truncated $\beta 5$ subunit is considered non-functional.

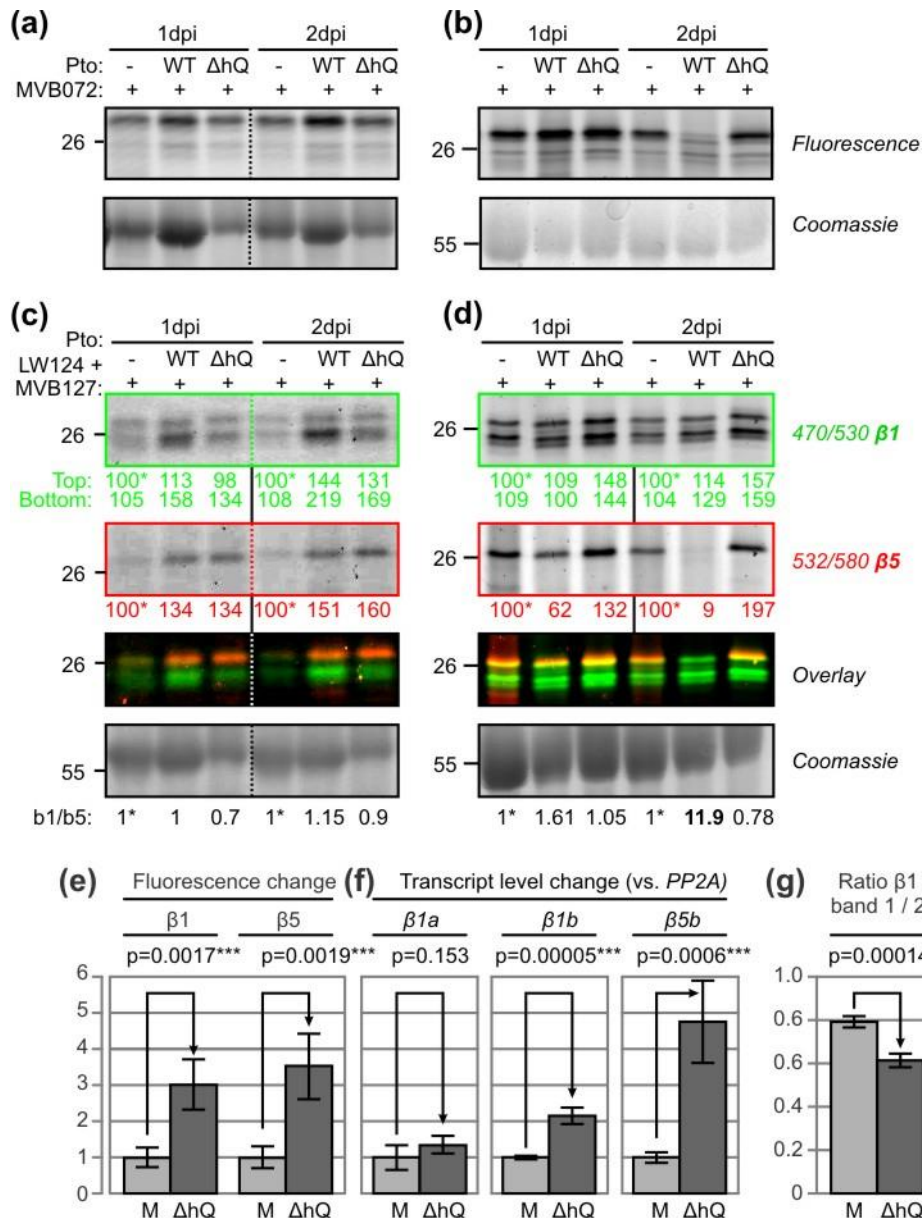


Figure 6. Uncoupled differential $\beta 1$ and $\beta 5$ activities upon bacterial infections.

(a-g) *N. benthamiana* leaves were infiltrated with buffer or 10^6 CFU/mL PtoDC3000(WT) or its derived $\Delta hopQ1-1$ mutant PtoDC3000(ΔhQ) and leaf disks were harvested at 1 and 2 dpi. Leaf extracts were labeled with MVB072 (a,b) or LW124+MVB127 (c,d) and proteins were analyzed as described in Figure 1b. Shown are representatives of independent experiments showing the two different phenotypes, ranging from induced $\beta 1/\beta 5$ activities (a,c; Supplemental Figures S4-S5), to suppressed $\beta 5$ activities (b,d; Supplemental Figures S6-S8). (e) Quantified fluorescence for $\beta 1$ (LW124) and $\beta 5$ (MVB127) in one experiment with four individuals (n=4 replicates). This experiment was reproduced twice with similar results (Supplemental Figures S9). (f) Relative transcript levels of $\beta 1a$, $\beta 1b$ and $\beta 5b$ relative to *PP2A* for the same experiment (n=4 individual plants) as shown in (e). (g) Relative ratio of the two LW124 signals in the same experiment (n=4 replicates) as shown in (e). This experiment was reproduced twice with similar results (Supplemental Figure S9).

SUPPLEMENTAL FIGURES

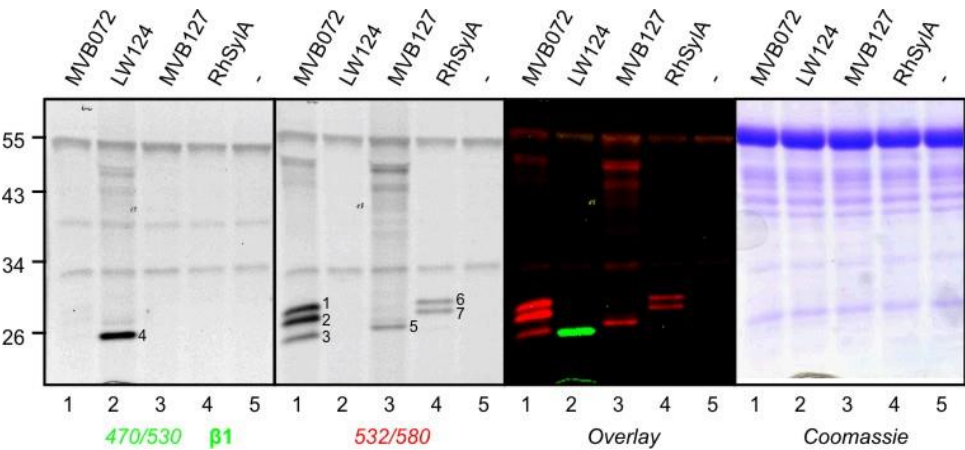


Figure S1. Entire gel showing selective labeling by different proteasome probes.

See legend of **Figure 1b** for more information

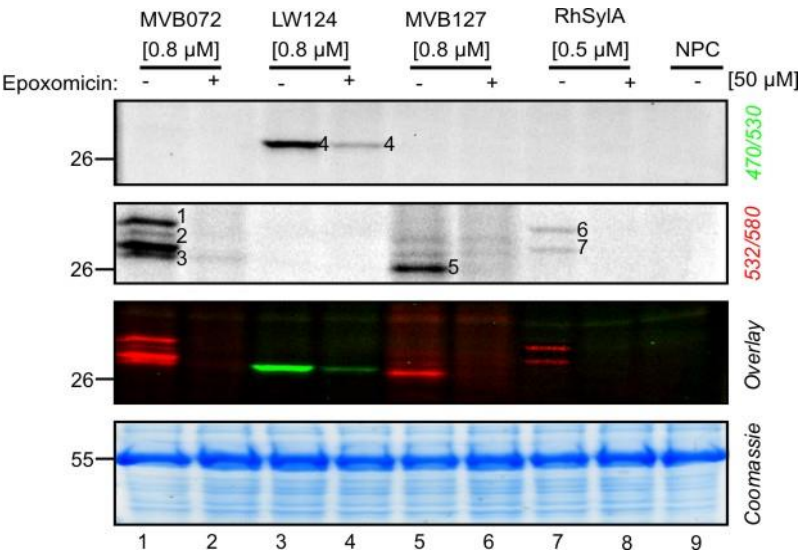


Figure S2. Labeling is blocked by pre-incubation with epoxomicin.

Arabidopsis leaf extracts were pre-incubated with 50 μ M epoxomicin for 30 min and labeled with MVB072, LW124, MVB127 and RhSylA. Fluorescent proteins were detected at two indicated settings of the fluorescence scanner. Numbers on gels annotate different signals caused by labeled proteasome subunits.

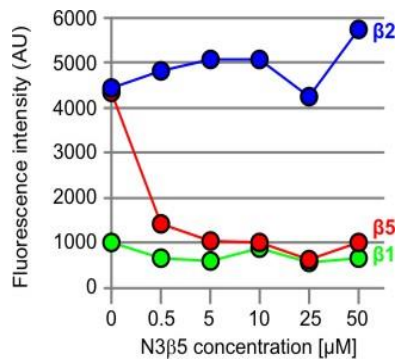


Figure S3. Selective $\beta 2$ labeling using [RhSylA + N3 $\beta 5$]

Arabidopsis leaf extracts were pre-incubated with increasing concentrations of the $\beta 5$ selective inhibitor N3 $\beta 5$ for 15 min followed by labeling with 0.5 μ M RhSylA for 30 min. Proteins were detected by in-gel fluorescent scanning and Sypro Ruby staining. Fluorescent signals corresponding to the catalytic subunits $\beta 1$, $\beta 2$ and $\beta 5$ were quantified from fluorescent gels. Fluorescence intensity values were normalized for loading using the Sypro Ruby signal. Values for the catalytic subunits were plotted against different N3 $\beta 5$ concentrations.

Beta 1

>MER412180 - Nbs00038021g0002.1
 MCIFISDSDESHQSN[TTSIVGVTYDDGVILGSTDITQLTANVFLCHCALGAYTQVLEEDARNFLDQETTAVA AEIVGMLLSAYDINNKNM
 LRTGVLLGGWDKNNGGKIYEIGFSGVMEKSNFGVGGYGTVDLNDFLEKEWKKGMT EEEAEQLVVKALSINNINS GCGVQTASVNSKEFTTAFH
 PYATLPIKA EKLESEHMNEKPMLECI RAHLLLLLLNINEGL

>MER411609 - Nbs00006786g0001.1
 MCIFIIDSEKSHQSN[TTSIVGVTYDDGVILGSTDITKTASVFLCHCALGADTQVLEEDARNFLDQETTATVA AEIVGMVLSAYDINNKNM
 LRTGVLLGGWDKNNGGKIYEIGFSGVMEKSNFGVGGYGAVDLNDFLEKEWKKGLT EEEAEQLVVKALSINNINS GCGAQTASVNSKGFTTDF
 HPYVILP IKA EKLELENMNEKPMLECI RAHLLLLLLNIDEGL

>MER412281 - Nbs00011733g0005.1 coverage after T:
 MDKSLLDVEQAHS MG[TIIGVTYNGRVVLGANSRTSTGMYVANRASDKITQLTDNVYVCRSGSAADSQVVS DYVRYFLHQHMIQLGQPATVKVA
 ANLVRLLSYNNKAM LQTGMIVGWDKYEGVKYMGFLLGAHSWNSLLLEVCQSVLFEYLILLPRSTLLVN

>MER412197 - Nbs00009991g0103.1 - β1a coverage after T:
 MDKSLLDVEQPHSMG[TIIGVTYNGGVVLGADSRSTSTGMYVANRASDKITQLTDNVYVCRSGSAADSQVVS DYVRYFLHQHTIQLGQPATVKVA
 ANLVRLLSYNNKAM LQTGM IIGWDKYEGGK[TYGVPLGGTLL EQPFAIGSGSSYLYGFFDQAWREGMTQEEAEKL VVTAVSLAIARDGASGGV
 VRTVTINKDGVTRKFYPGDTLPLWHEEIEAVNSLLDIVPAASPEPMVS

>MER411801 - Nbs00001896g0032.1 - β1b coverage after T:
 MENTDQVDPHSMG[TIIGVTYNGGVVLGADSRSTSTGMYVANRASDKITQLTDNVYVCRSGSAADSQIVSDYVRYFLHQHTIQLGQPATVKVAAN
 LTRLQTGM IIGWDKYEGGK[TYGIPLGGTVLEQPF AIGSGSSYLYGFFDQAWKEGMTQEEAEKL VVTAVSLAIARDGASGGVVRTVTINKDGA
 TRKFYPGDSLQLWHEELEPVNSLLDVVSASSPDPMVS

>MER411773 - Nbs00053861g0004.1 coverage after T:
 MENTDQVDPHSMG[TIIGVTYNGGVVLGADSRSTSTGMYVANRASDKITQLTDNVYVCRSGSAADSQIVSDYVRYFLHQHTIQLGQPATVKVAAN
 LTRLQLTGM IIGWDKYEGGK[TYGIPLGGTVLEQPF AIGSGSSYLYGFFDQAWKEGMTQEEAEKL VVTAVSLAIARDGASGGVVRTVTINKDGA
 TRKFYPGDSLQLWHEELEPVNSLLDVVSASSPDPMVS

Beta 2

>MER411637 - Nbs00015516g0007.1 - β2a coverage after T:
 MASKAATDVPMKGGFSFDLCRRNEMLVNKLGRSPSFLKTG[TIVGLIFQDGVILGADTRATEGP IIVADKNCEKIH YMAPNIYCCGAGTAADTEA
 VTD MVSSQLKLHRYHTGRESRVVTALTLKSHLFSYQGYVSAALVLGGVDVTGPHLHTIYPHGSTD TLPYATMGSGSLAAMAFESKYREGLSK
 DEG I K[LVAEAILSGVFNDLGSGSNVDICITKGNTEYLRNHMLPNPRTYPQKEVLLTKITPLRERFEVIEGGDAMEE

>MER411855 - Nbs00020859g0017.1
 MTAKATMDVPQKGGFSFDLCRRNEMLVNKLGRSPSFLKTG[TIVGLIFQDGVILGADTRATEGP IIVADKNCEKIH YMAPNIYCCGAGTAADTEA
 VTD MVSSQLKLHRYHTGRESRVVTALTLKSHLFSYQGHVSAALVLGGVDVTGPHLHTIYPHGSTD TLPYATNGLWFP RSNGL

>MER411772 - Nbs00022575g0009.1 - β2b coverage after T:
 MTAKATMDVPQKGGFSFDLCRRNEMLVNKLGRSPSFLKTG[TIVGLIFQDGVILGADTRATEGP IIVADKNCEKIH YMAPNIYCCGAGTAADTEA
 VTD MVSSQLKLHRYHTGRESRVVTALTLKSHLFSYQGHVSAALVLGGVDVTGPHLHTIYPHGSTD TLPYATMGSGSLAAMAFESKYREGMNR
 DEG I K[LVAEAILSGVFNDLGSGSNVDICITKGNTEYLRNHMLPNPRTYPQKGYSPFK[KTEVLLTKITPLRERFEVIEGGDAMEE

Beta 5

>MER412029 - Nbs00003340g0007.1 - β5b coverage after T:
 MMKIDFSGLEPTAPLKGESSVLC D GILSSPSFQIPNTNKEAIQMVKPAKG[TTLAFIFKGGVMVAADSRASMG GYISSQSVKKIIEINPYMLG
 TMAGGAADCQFWHRNLGIKENANFVAIVILIDHGLYKCCWPILKEDLIAVLEHLYKEGKEKNWMIVRGICAGWILLVVELCVVCR LH
 MGLSVGTMIAGWDEKGPGLYYVDSEGGRLKGNRFSVSGSGSPYAYGVLD SGYRFDLSVEEAAELARRAIYHATFRD GASGGVASVYHVGPNGWK
 LSGDDV GELHYNYPVELESVEQEMAEPVA

>MER411662 - Nbs00002652g0001.1 - β5a coverage after T:
 MMKIDFSGLEPTAPIKGESELCDGILSSPSFQIPNATNFDGFGKEAIQMVKPAKG[TTLAFIFKGGVMVAADSRASMG GYISSQSVKKIIEIN
 PYMLGTMAGGAADCQFWHRNLGIKENANFVAIVILIDHGLYKCCWPILKEDLIAVLEHLYKEGKEKNWMIVRGICAGWILLVVELCVVCR LH
 ELANKRRISVAGASKLLANILYSYRGMGLSVGTMIAGWDEKGPGLYYVDSEGGRLKGNRFSVSGSGSPYAYGVLD SGYRFDLSVEEAAELARRAI
 YHATFRD GASGGVASVYHVGPNGWK[LSGDDV GELHYSYYPVELESVEQEMAEPVA

>MER412196 - Nbs00002498g0003.1 coverage after T:
 MMKIDFSGLEPTAPIKGESELCDGILSSPSFQIPNATNFDGFGKEAIQMVKPAKG[TTLAFIFKGGVMVAADSRASMG GYISSQSVKKIIEIN
 PYMLGTMAGGAADCQFWHRNLGIKCR LHELANKRRISVAGASKLLANILYSYRGMGLSVGTMIAGWDEKGPGLYYVDSEGGRLKGNRFSVSGSGS
 PYAYGVLD SGYRFDLSVEEAAELARRAIYHATFRD GASGGVASVYHVGPNGWK[LSGDDV GELHYNYPVELESVEQEMAEPVA

Figure S3. Identified peptides mapped on the protein sequences of the catalytic subunits of the *N. benthamiana* proteasome. Shown are the catalytic Thr (blue); unique peptides (red); peptides shared by two proteins (dark grey); peptides shared by more than two proteins (light grey); peptides that overlap with a larger peptide (missed cleavage, underlined). Subunits that are too short are printed with grey letters.

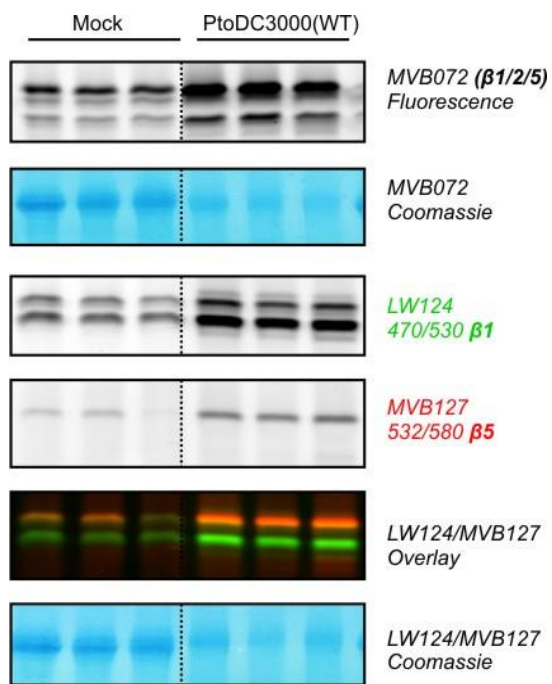


Figure S4. Increased proteasome activity upon WT infection. Shown is one experiment containing three biological replicates.

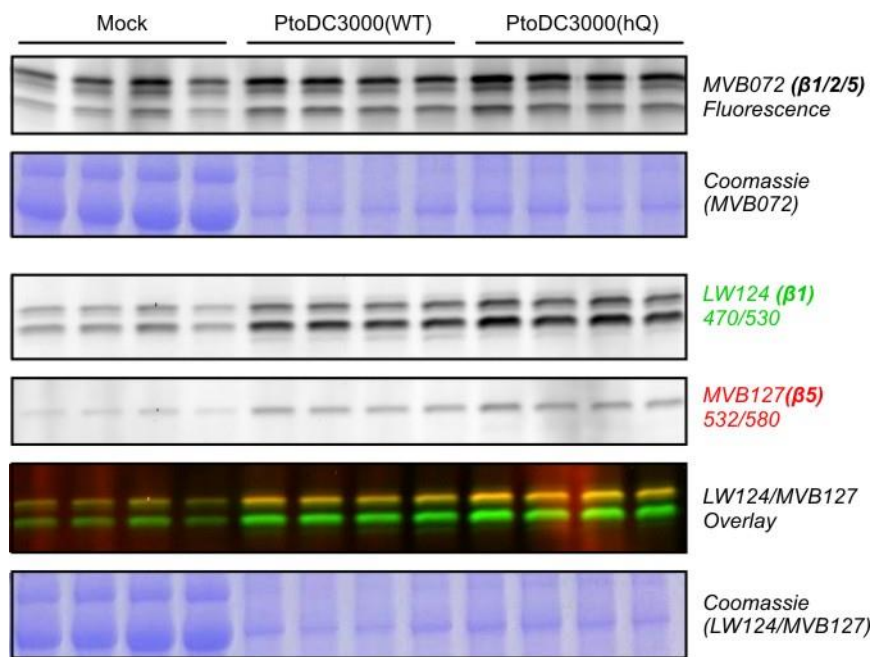


Figure S5. Increased proteasome activity upon WT infection. Shown is one experiment containing four biological replicates. See **Figure 6** for more details.

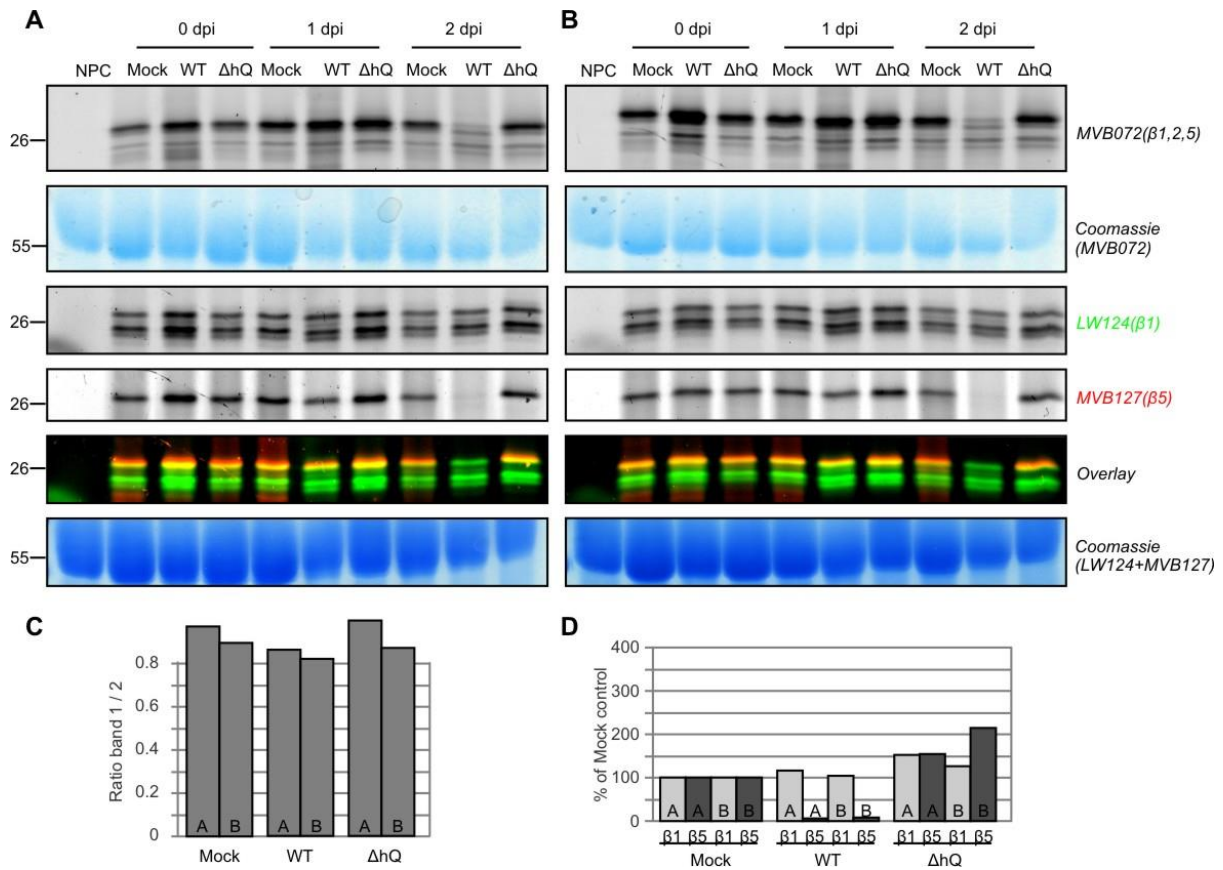


Figure S6. Suppressed $\beta 5$ labeling upon WT infection. **A, B**) Shown is one experiment containing two biological replicates. Part of the right half of this figure is shown in **Figure 6bd**. **C**) Ratio of the two $\beta 1$ signals. **D**) Fluorescent intensity of the signals, normalized to the Mock control. See Figure 6 for more details.

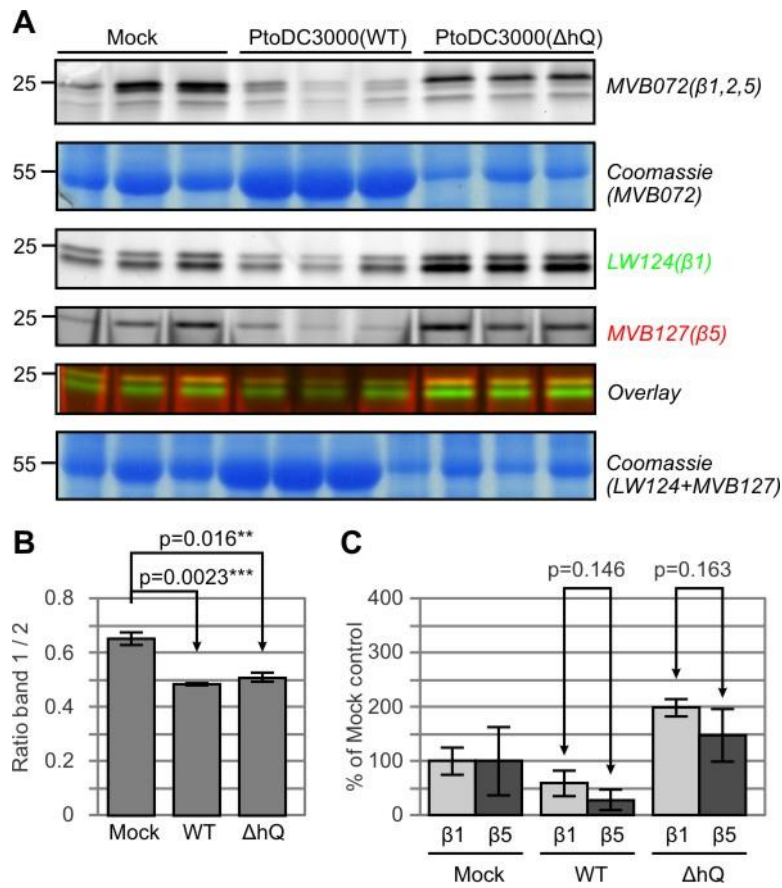


Figure S7. Suppressed β 5 labeling upon WT infection. Shown is one experiment containing three biological replicates. **B)** Ratio of the two β 1 signals. **C)** Fluorescent intensity of the signals, normalized to the Mock control. See Figure 6 for more details.

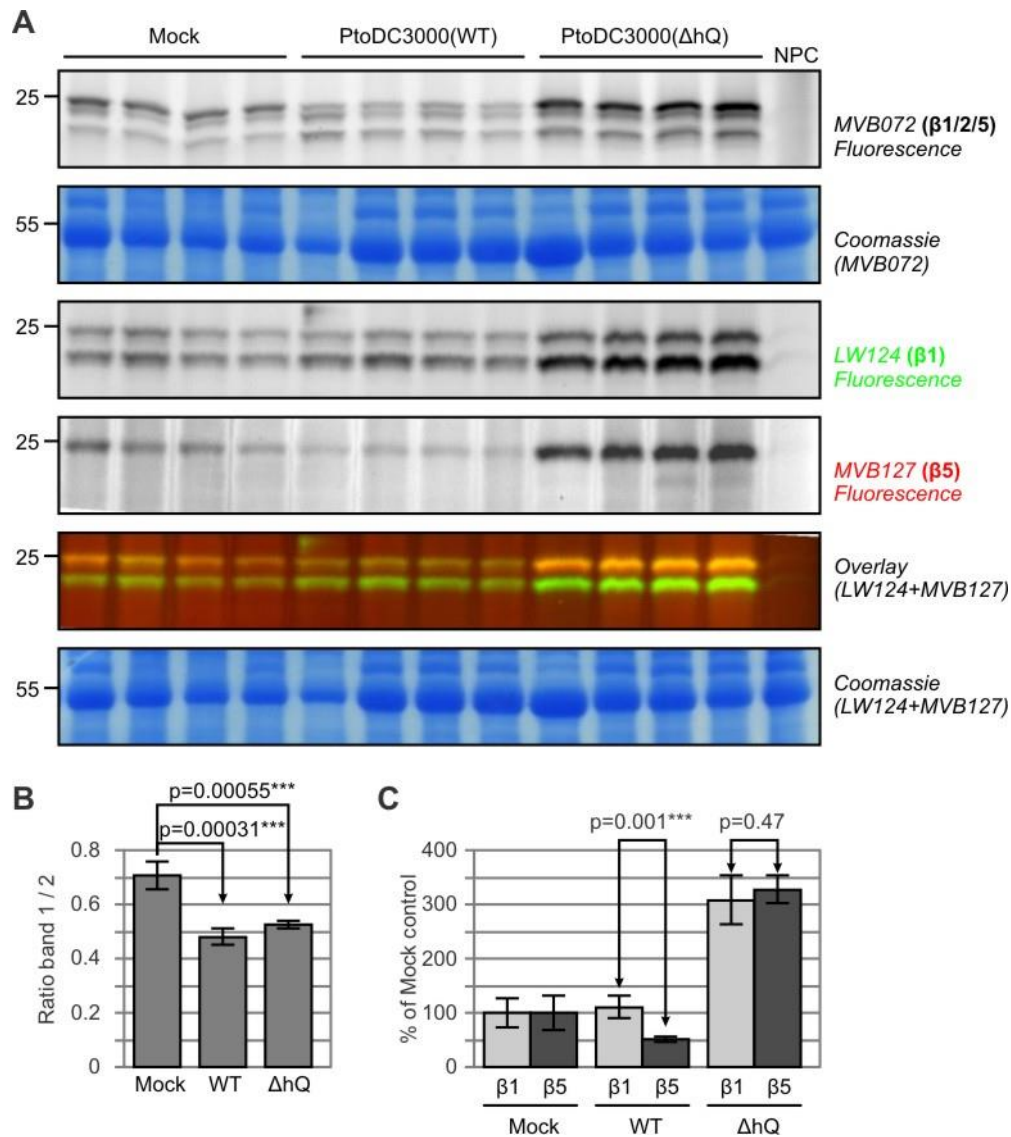


Figure S8. Suppressed β5 labeling upon WT infection. Shown is one experiment containing four biological replicates. **B)** Ratio of the two β1 signals. **C)** Fluorescent intensity of the signals, normalized to the Mock control. See Figure 6 for more details.

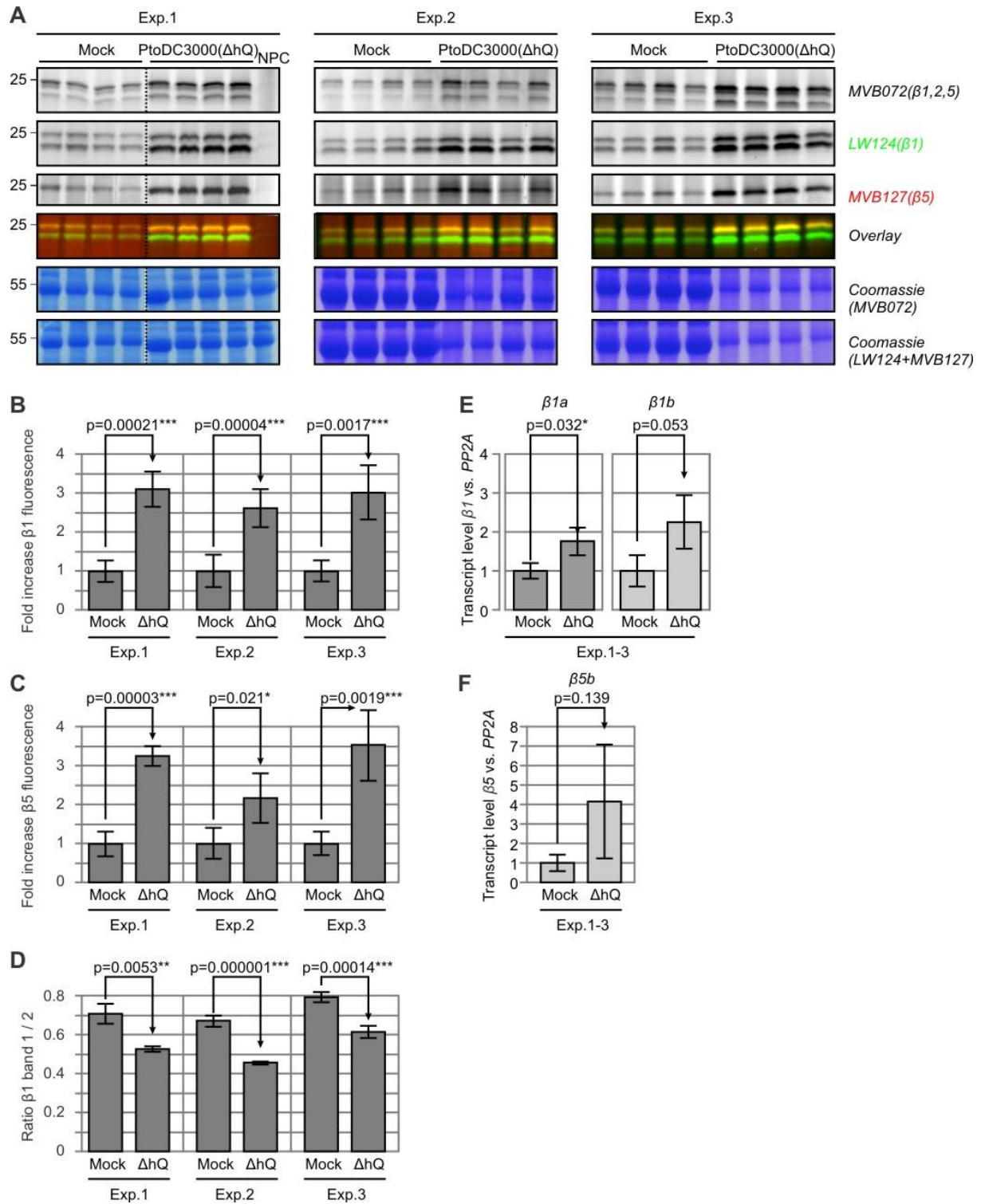


Figure S9 Altered proteasome activity upon infection with PtoDC3000(Δ hQ). **A**) Shown are three independent experiments, each containing four biological replicates. **B, C**) Fluorescence intensity normalized to the Mock control for each of the three experiments. **D**) Ratio of β 1 signals 1 and 2 for each of the three experiments. **E, F**) qRT-PCR, performed on the three biological experiments. Replicates of each biological experiment were mixed ($n=4$) and the average of expression and standard deviation were calculated for the three biological experiments. See **Figure 6** for more details.

901 **Table S1:** Identified peptides of catalytic subunits*.

Peptide sequence	u/s	score	protein	BTH		H2O	
				MS1	MS2	MS1	MS1
EGMTQEAEK	s	175.5	beta 1	2	2	2	2
FYPGDSLQLWHEELEPVNSLLDVVSASSPDPMS	s	110.2	beta 1	1	0	2	0
ITQLTDNVYVCR	s	283.5	beta 1	4	3	4	4
IYGIPLGGTVLEQPFAGGSGSSYLYGFFDQAWK	s	155.5	beta 1	2	1	2	1
KFYPGDSLQLWHEELEPVNSLLDVVSASSPDPMS	s	57.14	beta 1	1	0	2	0
LLSYNNK	s	128.5	beta 1	1	1	1	1
LQTGMIIGGWDK	s	151.7	beta 1	3	2	3	3
LVVTAVSLAIAR	s	168.0	beta 1	3	2	2	2
SGSAADSQIVSDYVR	s	254.9	beta 1	2	3	3	1
SGSAADSQVVS DYVR	s	299.2	beta 1	2	2	2	2
TSTGMYVANR	s	228.2	beta 1	5	5	6	5
VAANLVR	s	137.8	beta 1	1	1	1	1
YFLHQHTIQLGQPATVK	s	298.1	beta 1	3	4	4	3
ATEGPIVADK	s	199.3	beta 2	2	3	2	2
ATEGPIVADKNCEK	s	177.0	beta 2	0	0	1	0
GNTEYLR	s	129.7	beta 2	1	1	1	1
IHYMAPNIYCCGAGTAADTEAVTDMVSSQLK	s	138.4	beta 2	1	0	3	0
IIEINPYMLGT MAGGAADCQFWHR	s	103.6	beta 2	2	1	3	0
AIYHATFR	s	204.8	beta 5	1	0	1	0
ASMGYISSQSVK	s	214.6	beta 5	6	4	4	5
DGASGGVASVYHVGPNGWK	s	287.0	beta 5	4	2	4	2
FDLSVEEAAELAR	s	373.7	beta 5	3	4	2	3
FSVSGSPYAYGVLD SGYR	s	242.7	beta 5	4	5	6	5
GGVMVAADSR	s	123.0	beta 5	3	3	3	5
GMGLSVGTMIAGWDEK	s	214.9	beta 5	7	4	8	6
GPGLYYVDSEGR	s	136.9	beta 5	1	1	2	2
ISVAGASK	s	124.1	beta 5	0	0	1	0
KLSGDDVGLHYNYPVELESVEQEMAEVPVA	s	57.9	beta 5	2	0	2	0
LHELANK	s	141.0	beta 5	2	1	1	1
LHELANKR	s	141.5	beta 5	1	1	1	0
LLANILYSYR	s	190.6	beta 5	1	1	1	2
LSGDDVGLHYNYPVELESVEQEMAEVPVA	s	68.84	beta 5	2	2	4	2
RAIYHATFR	s	128.5	beta 5	1	0	1	0
RISVAGASK	s	120.6	beta 5	0	0	1	0
ITQLNDNVYVCR	u	218.0	Nbs00001896g0032.1	1	1	2	1
KLSGDDVGLHYSYPVELESVEQEMAEVPVA	u	50.03	Nbs00002652g0001.1	0	0	1	0
IYGVPLGGTLLEQPFAGGSGSSYLYGFFDQAWR	u	111.2	Nbs00009991g0103.1	0	1	0	1
ERVEIEGGDAMEE	u	197.1	Nbs00015516g0007.1	1	0	1	0
NHMLPNR	u	94.16	Nbs00015516g0007.1	1	0	1	0
LVAEAILSGVFNDLGSGSNVDICIITK	u	112.5	Nbs00015516g0007.1	1	1	0	0
VEVIEGGDAMEE	u	202.0	Nbs00015516g0007.1	1	0	1	0
KTEVLLTK	u	181.5	Nbs00022575g0009.1	2	1	2	1
EIVQVIEGGDAMEE	u	227.6	Nbs00022575g0009.1	5	1	4	1
LVAEAILSGVFNDLGSGSNVDICVITK	u	119.2	Nbs00022575g0009.1	1	1	1	0
TEVLLTK	u	143.6	Nbs00022575g0009.1	2	1	2	1

902 *, unique (u) or shared (s); highest peptide score; protein hit; spectral counts in the two pull down
903 experiments, each analyzed twice by MS.